

Genetic and Functional Studies Implicate Synaptic Overgrowth and Ring Gland cAMP/PKA Signaling Defects in the *Drosophila melanogaster* Neurofibromatosis-1 Growth Deficiency

James A. Walker^{1,2}, Jean Y. Gouzi^{1✉a}, Jennifer B. Long³, Sidong Huang^{4✉b}, Robert C. Maher¹, Hongjing Xia¹, Kheyal Khalil¹, Arjun Ray¹, David Van Vactor³, René Bernards⁴, André Bernards^{1,2✉b*}

1 Massachusetts General Hospital Center for Cancer Research and Harvard Medical School, Charlestown, Massachusetts, United States of America, **2** Center for Human Genetic Research, Massachusetts General Hospital, Boston, Massachusetts, United States of America, **3** Department of Cell Biology, Harvard Medical School, Boston, Massachusetts, United States of America, **4** Division of Molecular Carcinogenesis, The Netherlands Cancer Institute, Amsterdam, The Netherlands

Abstract

Neurofibromatosis type 1 (NF1), a genetic disease that affects 1 in 3,000, is caused by loss of a large evolutionary conserved protein that serves as a GTPase Activating Protein (GAP) for Ras. Among *Drosophila melanogaster* *Nf1* (*dNf1*) null mutant phenotypes, learning/memory deficits and reduced overall growth resemble human NF1 symptoms. These and other *dNf1* defects are relatively insensitive to manipulations that reduce Ras signaling strength but are suppressed by increasing signaling through the 3'-5' cyclic adenosine monophosphate (cAMP) dependent Protein Kinase A (PKA) pathway, or phenocopied by inhibiting this pathway. However, whether *dNf1* affects cAMP/PKA signaling directly or indirectly remains controversial. To shed light on this issue we screened 486 1st and 2nd chromosome deficiencies that uncover >80% of annotated genes for dominant modifiers of the *dNf1* pupal size defect, identifying responsible genes in crosses with mutant alleles or by tissue-specific RNA interference (RNAi) knockdown. Validating the screen, identified suppressors include the previously implicated *dAlk* tyrosine kinase, its activating ligand *jelly belly* (*jeb*), two other genes involved in Ras/ERK signal transduction and several involved in cAMP/PKA signaling. Novel modifiers that implicate synaptic defects in the *dNf1* growth deficiency include the intersectin-related synaptic scaffold protein Dap160 and the cholecystokinin receptor-related CCKLR-17D1 drosulfakinin receptor. Providing mechanistic clues, we show that *dAlk*, *jeb* and *CCKLR-17D1* are among mutants that also suppress a recently identified *dNf1* neuromuscular junction (NMJ) overgrowth phenotype and that manipulations that increase cAMP/PKA signaling in adipokinetic hormone (AKH)-producing cells at the base of the neuroendocrine ring gland restore the *dNf1* growth deficiency. Finally, supporting our previous contention that ALK might be a therapeutic target in NF1, we report that human ALK is expressed in cells that give rise to NF1 tumors and that NF1 regulated ALK/RAS/ERK signaling appears conserved in man.

Citation: Walker JA, Gouzi JY, Long JB, Huang S, Maher RC, et al. (2013) Genetic and Functional Studies Implicate Synaptic Overgrowth and Ring Gland cAMP/PKA Signaling Defects in the *Drosophila melanogaster* Neurofibromatosis-1 Growth Deficiency. PLoS Genet 9(11): e1003958. doi:10.1371/journal.pgen.1003958

Editor: Gregory P. Copenhaver, The University of North Carolina at Chapel Hill, United States of America

Received December 7, 2012; **Accepted** October 1, 2013; **Published** November 21, 2013

Copyright: © 2013 Walker et al. This is an open-access article distributed under the terms of the Creative Commons Attribution License, which permits unrestricted use, distribution, and reproduction in any medium, provided the original author and source are credited.

Funding: JAW, RCM, HX, KK, AR and AB were supported by NIH/NGMS grant 1-R01 GM084220. AB also received support from an anonymous donor. JYG was supported by Young Investigator Award from the Children's Tumor Foundation. SH and RB were supported by Dutch cancer society grant NKI 2009-4496. The funders had no role in study design, data collection and analysis, decision to publish, or preparation of the manuscript.

Competing Interests: The authors have declared that no competing interests exist.

* E-mail: abernards@helix.mgh.harvard.edu

✉a Current address: Institute of Cellular and Developmental Biology, Biomedical Sciences Research Centre "Alexander Fleming," Vari, Greece.

✉b Current address: Department of Biochemistry, McIntyre Medical Building, Montreal, Quebec, Canada.

Introduction

RASopathies, caused by mutations that activate Ras/ERK signaling, are a group of related disorders with features that include facial dysmorphisms, skeletal, skin and cardiac defects, cognitive deficits, reduced growth and an increased cancer risk [1]. Neurofibromatosis type 1 (NF1; OMIM 162200), caused by loss of a RasGAP, and Noonan syndrome, caused by mutations that alter Ras/ERK pathway proteins SOS1, KRAS, NRAS, RAF1, BRAF, CBL, PTPN11, or SHOC2, are the most common members of this group, affecting 1 in 3,000, or as many as 1 in 1,000 live births, respectively [2,3]. The genetics of these disorders provides a strong argument that excess Ras/ERK signaling underlies

common RASopathy symptoms, and much effort remains focused on attenuating Ras/ERK signaling as a strategy for therapeutic intervention. However, whether life-long pharmacological inhibition of Ras/ERK signaling is a viable strategy to treat the full range of often non-life-threatening, but nonetheless serious symptoms of these chronic disorders, remains an open question. This motivates our work to better understand the molecular and cellular pathways responsible for NF1 symptom development, in the hope this will identify more specific therapeutic targets.

We have been interested in using *Drosophila melanogaster* as a model to investigate NF1 functions *in vivo*, following our identification of a conserved *dNf1* ortholog predicting a protein that is 60% identical to human neurofibromin over its entire 2802

Author Summary

Neurofibromatosis type 1 (*NF1*) is a genetic disease that affects 1 in 3,000 and that is caused by loss of a protein that inactivates Ras oncproteins. *NF1* is a characteristically variable disease that predisposes patients to several symptoms, the most common of which include benign and malignant tumors, reduced growth and learning problems. We and others previously found that fruit fly mutants that lack a highly conserved *dNf1* gene are reduced in size and exhibit impaired learning and memory, and that both defects appear due to abnormal Ras and cyclic-AMP (cAMP) signaling. The former was unremarkable, but how loss of *dNf1* affects cAMP signaling remains poorly understood. Here we report results of a genetic screen for dominant modifiers of the *dNf1* growth defect. This screen and follow-up functional studies support a model in which synaptic defects and reduced cAMP signaling in specific parts of the neuroendocrine ring gland contribute to the *dNf1* growth defect. Beyond these results, we show that human ALK is expressed in cells that give rise to *NF1* tumors, and that *NF1* regulated ALK/RAS/ERK signaling is evolutionary conserved.

amino acid length [4]. Like human neurofibromin, the Drosophila protein functions as a GAP for conventional (*dRas1*) and R-Ras-like (*dRas2*) GTPases [4,5]. This functional conservation made it all the more surprising when both initially identified *dNf1* homozygous null mutant phenotypes, a postembryonic growth deficiency and a neuropeptide-elicited NMJ electrophysiological defect, appeared insensitive to genetic manipulations that attenuate Ras signaling strength, but were suppressed by increasing signaling through the cAMP-dependent PKA pathway [4,6]. The genetic link between *dNf1* and cAMP/PKA led to further studies, which demonstrated that similar to many children with *NF1* [7], and *Nf1*^{+/−} mice [8], *dNf1*^{−/−} flies exhibit specific learning and memory deficits [9]. Biochemical studies with fly brain extracts further revealed that loss of *dNf1* is associated with reduced GTP-γS-stimulated but not basal adenylyl cyclase (AC) activity [9], and with defects in both classical and unconventional AC pathways [10]. Arguing that the cAMP related function of *NF1* is evolutionary conserved, GTP-γS-stimulated AC activity and cAMP levels were also reduced in E12.5 *Nf1*^{−/−} mouse brain [11], and defects in cAMP generation appear to explain the unique sensitivity to *Nf1* heterozygosity of murine central nervous system neurons [12]. Arguing that *NF1* may regulate cAMP signaling at least in part in a cell autonomous manner, reduced cAMP levels and AC activity were also found in *Nf1* deficient human astrocytes [13]. Thus, while there is little doubt that aberrant AC signaling is an evolutionary conserved *NF1* phenotype, we and others have reached conflicting conclusions about the underlying mechanism.

Based on Drosophila phenotypic rescue studies with human *NF1* transgenes, others reported that neurofibromin has physically separable functions as a negative regulator of Ras and a positive mediator of AC/PKA signaling. This conclusion followed from findings that *NF1*-GAP activity was not required to rescue *dNf1* size [10] or learning [14] phenotypes, whereas a transgene encoding a C-terminal part of human neurofibromin that did not include the GAP catalytic domain did suppress both defects. In obvious conflict, in similar experiments with *dNf1* transgenes, we found that neuronal expression of a functional *NF1*-GAP catalytic segment was necessary and sufficient to suppress the systemic growth defect, and that other protein segments had no effect.

Moreover, the *dNf1* growth defect was also suppressed by neuronal expression of the Drosophila p120RasGAP ortholog, and although we extended earlier findings by showing that heterozygous loss of *dRas1* or *dRas2*, or of a comprehensive set of Ras effector proteins did not modify the growth defect, these mutations also did not reduce the elevated phospho-ERK level in the *dNf1* central nervous system (CNS). However, some Ras/ERK signaling is the proximal cause of the non-cell-autonomous *dNf1* growth defect [5]. Further supporting this notion, recent work implicated the neuronal *dAlk* tyrosine kinase receptor and its activating ligand *jelly belly* (*jeb*) as rate-limiting activators of *dNf1* regulated Ras/ERK pathways responsible for both systemic growth and olfactory learning defects [15].

The above evidence underlies our hypothesis that loss of *dNf1* increases neuronal *dAlk*/Ras/ERK activity, which in turn causes reduced cAMP/PKA signaling, which may or may not be cell-autonomous. Obviously, identifying additional components of *dNf1*-regulated growth controlling pathways followed by functional analysis might help to test this hypothesis. Here we report results of a *dNf1* growth deficiency modifier screen, which identified components of tyrosine kinase/Ras/ERK and neuropeptide/cAMP/PKA pathways in addition to genes involved in synaptic morphogenesis and functioning. Further analysis showed that the requirement for *dNf1* and cAMP/PKA in Drosophila growth regulation involves different tissues, with *dNf1* required broadly in larval neurons, and cAMP/PKA signaling specifically in AKH-producing cells and perhaps in other parts of the neuroendocrine ring gland. These results, and the recent discovery of a novel *dNf1* synaptic overgrowth phenotype [16] that is also suppressed by several genes identified in our screen, set the stage for further work to more precisely define how loss of *dNf1* causes Ras/ERK and other signaling defects, the ultimate consequence of which is reduced systemic growth.

Results

Loss of *dNf1* Does Not Phenocopy Starvation or Alter Developmental Timing

Animals use elaborate hormonal mechanisms to coordinate nutrient availability and feeding with changes in metabolism and overall growth. Since starvation or crowding during the larval phase of the Drosophila life cycle reduces systemic growth [17], we first examined whether the small size of *dNf1* mutants reflected reduced feeding. Arguing against this hypothesis, wild-type and *dNf1* larvae ingested similar amounts of dye-stained food throughout their development (Figure 1A). Unlike a *pumpless* (*ppl*) mutant [18], *dNf1* larvae also showed no tendency to move away from a food source (Figure 1B). Analysis of the expression of the starvation-inducible *Pepck* and *Lip3* genes [18] provided further evidence that loss of *dNf1* does not phenocopy starvation (Figure 1C).

Mechanisms that control Drosophila growth have been the topic of intense study and much has been learned about how an interplay between insulin-like peptide (ILP) controlled growth rate and ecdysone controlled growth duration determines overall growth (see [19] and [20] for reviews). Arguing against an important role for ecdysone or other factors that control the length of the larval growth period, no differences in the expression of canonical ecdysone-regulated genes was found (results not shown) and no difference in developmental timing between wild-type and *dNf1* mutants was detected (Figure 1D and S1). Rather, a reduced growth rate throughout larval development results in an approx-

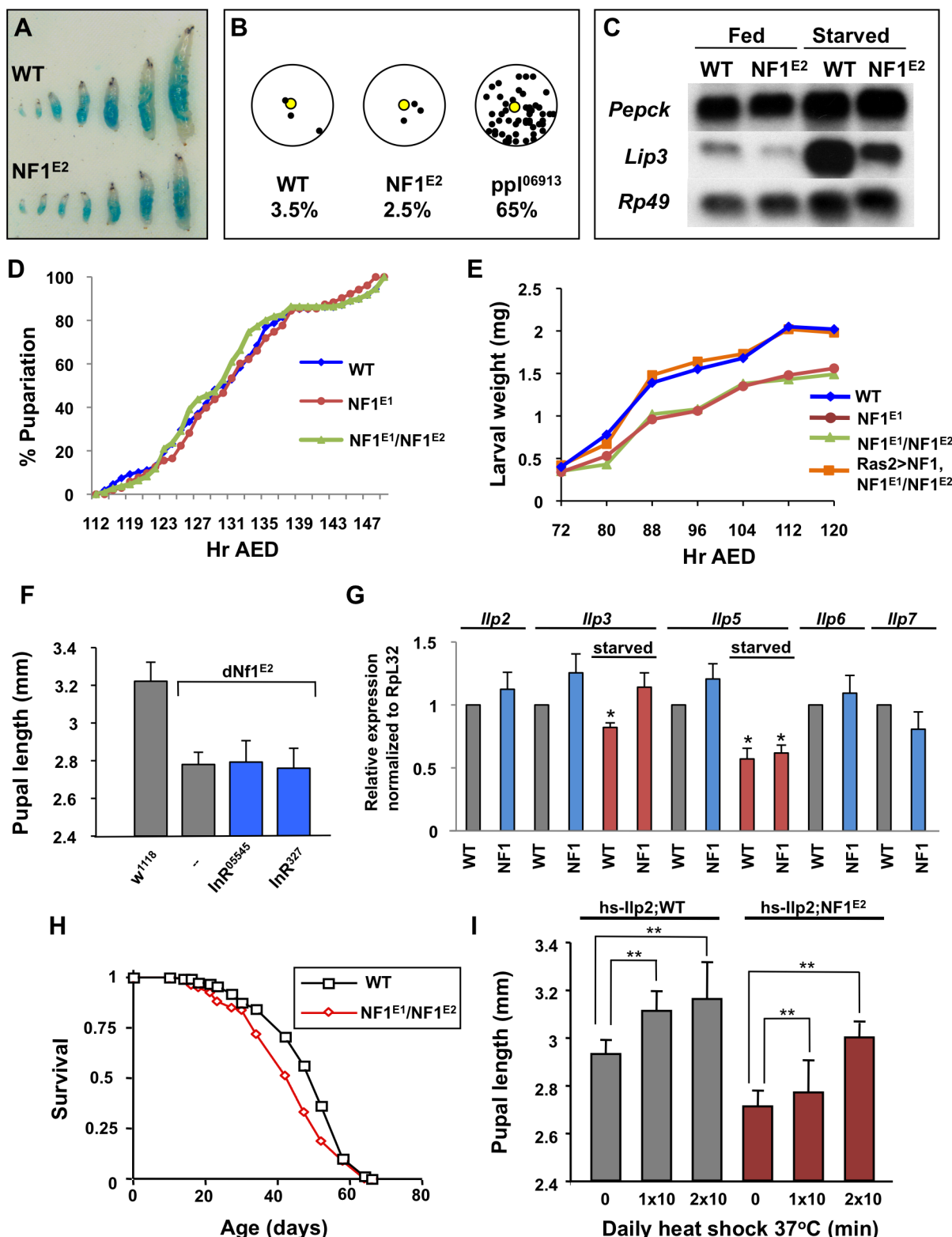


Figure 1. Loss of *dNf1* does not phenocopy starvation or alter developmental timing. (A) Wild-type (*w¹¹¹⁸*) and *dNf1* larvae ingest similar amounts of food. Larvae at different stages of development were photographed after 25 minutes of feeding on dye-colored yeast paste. (B) As opposed to *ppl* mutants, wild-type and *dNf1* larvae do not wander from a food source (fraction of wandering larvae: WT 3.5% (SD 0.007), *dNf1* 2.5% (SD 0.007) and *ppl* 65% (SD 0.057)). In a similar assay, *dNf1* larvae also showed no abnormality in moving towards a food source (not shown). (C) RNA blot analysis of the starvation-sensitive genes, *PEPCK* and *Lip3* shows that *dNf1* larvae do not show elevated levels of either mRNA under normal feeding conditions. (D) Wild-type and *dNf1* larvae show no significant differences in developmental timing, as assessed by time of pupariation after egg deposition (AED). (E) The *dNf1* growth rate, as assessed by larval weight, is reduced throughout larval development when compared to wild-type or a *Ras2>UAS-dNf1* control. (F) Two hypomorphic insulin receptor alleles, *InR⁰⁵⁵⁴⁵* and *InR³²⁷*, do not modify *dNf1* pupal size. (G) ILP mRNA expression

is not obviously reduced in *dNf1* larvae. H) *dNf1* adult flies show no altered longevity compared to wild-type controls. (I) Over-expression of *Ilp2* from a *hs-Ilp2* transgene in *dNf1* larvae results in a similar increase in size as in wild-type flies.
doi:10.1371/journal.pgen.1003958.g001

imately 25% weight reduction of *dNf1* pupae relative to isogenic controls (Figure 1E and S1).

Drosophila ILPs control systemic growth, metabolism, longevity, and female fecundity [21–24]. Among the eight Drosophila ILP genes, *Ilp2*, *Ilp3* and *Ilp5* are co-expressed in bilateral clusters of seven insulin-producing neurosecretory cells (IPCs) in the larval brain [21]. Ablation of these cells causes a severe reduction in overall size, which is rescued by inducing the expression of a *hsp70-Ilp2* transgene [22,23]. However, several results argue against a role for ILPs in the *dNf1* growth defect. Firstly, two hypomorphic insulin receptor alleles, *InR⁰⁵⁵⁴⁵* and *InR³²⁷*, did not affect *dNf1* pupal size (Figure 1F). Secondly, qRT-PCR analysis of RNA extracted from wandering wild-type and *dNf1* third instar larvae detected no major differences in the expression of *Ilp1* (not shown), *Ilp2*, *Ilp3*, *Ilp5*, *Ilp6* and *Ilp7* in fed larvae. Among the three IPC expressed ILP genes, the expression of *Ilp3* and *Ilp5* is reduced in response to starvation [21]. Starved wild-type and *dNf1* larvae showed a similar reduction in *Ilp5* expression, whereas *Ilp3* showed a less pronounced response (Figure 1G). Thirdly, while certain insulin receptor or insulin receptor substrate (*chico*) mutants have an up to 85% increased life span [25,26], the lifespan of *dNf1* mutants and isogenic controls was comparable (Figure 1H). We note that others previously reported a reduced life span for the originally identified *dNf1* p-element alleles, generated in a different genetic background [27]. Finally, we previously showed that *Ilp2-GAL4* driven *UAS-dNf1* expression in IPCs did not rescue the *dNf1* size defect [5]. Although daily heat shocking of *hsp70-Ilp2* carrying larvae increased the size of *dNf1* pupae, indicating that mutants do not lack the ability to respond to insulin, similar induction of this transgene, as previously noted [21], also substantially increased the size of wild-type controls (Figure 1I). Thus, reduced insulin signaling does not provide an obvious explanation for the slower *dNf1* growth rate, prompting us to perform a screen to identify other genes involved in *dNf1*-mediated systemic growth control.

Screen for Dominant Modifiers of *dNf1* Systemic Growth Phenotype

While most *dNf1* defects are poorly suited for use in modifier screens, the postembryonic growth defect is robust and readily quantified during the pupal stage [4]. However, using this phenotype in a screen is complicated by the fact that organismal size is sexually dimorphic (females are larger than males) and affected by population density, feeding, environmental factors and genetic background differences. With these confounding factors in mind, we used the crossing schemes outlined in Figure 2 to test collections of isogenic 1st and 2nd chromosome deficiencies for *dNf1^{E2}* pupal size modifier effects or synthetic lethal interactions. For each of 139 1st and 347 2nd chromosome deficiencies from the Exelixis [28], DrosDel [29] or Bloomington Stock Center (BSC) collections, we generated *Df(1)/+; Nf1^{E2}/Nf1^{E2}* (Figure 2A) or *Df(2)/+; Nf1^{E2}/Nf1^{E2}* (Figure 2B) stocks, respectively. Notably, our work identified only few synthetic lethal interactions, and in all cases tested the synthetic lethality has been specific to the chromosome carrying the *Nf1^{E2}* allele, and not observed when the same deficiency was tested in *Nf1^{E2}/Nf1^{E1}* null trans-heterozygotes [5]. To guard against size differences caused by inadvertent differences in population density or environmental conditions, each deficiency was scored at least twice using an initial rough caliper measurement of pupae attached to the side of culture vials. For each candidate modifying deficiency thus

identified, microscopy combined with image analysis was used to determine the precise head-to-tail length of at least 40 pupae, which were then allowed to individually eclose in order to establish their sex. Several controls were next performed to eliminate non-specific modifiers or artifactual results. First, for all suppressors the continued presence of the *Nf1^{E2}* nonsense mutation was confirmed by a PCR assay (Figure S2). Secondly, as a critical specificity control, all modifying deficiencies were analyzed in a wild-type background to eliminate those that affect pupal size irrespective of *dNf1* genotype. Further analysis of some of these non-specific modifiers demonstrated that loss of *Act57B* dominantly increases pupal size, whereas heterozygous loss of the glutamate transporter *Eaat1* has the opposite effect. Thirdly, because pupal size is a function of larval growth rate and duration, modifying deficiencies were monitored for obvious changes in developmental timing. Table 1 shows the number of screened chromosome 1, 2L and 2R deficiencies, the fraction of genes uncovered and the number of *dNf1* and wild-type pupal size modifying deficiencies and loci identified. Figure 2C shows the magnitude of the pupal size modification of typical enhancers and suppressors. The number of modifying deficiencies exceeds the number of identified loci, because many modifying deficiencies uncover overlapping genomic segments (Figure 3). Not unexpectedly, individual modifying deficiencies increase or decrease *dNf1* pupal size to different extents (Figure 4).

Some large non-modifying deficiencies identified in our screen completely overlapped with smaller modifying ones. In such cases, stocks were re-ordered and reanalyzed. If these tests replicated the original results, genetic complementation analysis or PCR amplification using transposon and flanking sequence-specific primers was used to confirm the mapping of the deficiencies in question. This procedure identified several mislabeled deficiencies, most of which have since been withdrawn by stock centers. Any suspect or recessive modifying deficiency, or any deficiency that uncovers genes with non-specific size phenotypes, such as *Minute* loci [30,31], were eliminated from further analysis. Table S1 lists these deficiencies and the reason for their exclusion.

During work to identify genes responsible for observed effects, we prioritized genes uncovered by suppressing deficiencies over those uncovered by enhancers. We also prioritized modifying loci uncovered by more than one deficiency, strong modifiers over weak ones, and genes uncovered by smaller deficiencies over those uncovered by larger ones, reasoning that effects of smaller deficiencies are more likely due to the loss of single genes. Validating the screen, suppressing *Df(2R)Exel7144* uncovers *dAlk* and partially overlapping suppressing *Df(2R)BSC199* and *Df(2R)BSC699* each uncover the gene for its activating ligand, *jeb*, both previously identified as dominant suppressors of *dNf1* size, learning, and neuronal ERK over-activation phenotypes [15]. Other uncovered candidate modifiers, such as PKA catalytic and regulatory subunit genes, were tested in crosses with loss-of-function alleles and/or by tissue-specific knockdown using at least two independent UAS-RNAi transgenes, most of which were obtained from the Vienna Drosophila Stock Center (VDRC) [32]. For deficiencies that lacked obvious candidate modifiers, we used the UAS-RNAi approach to more broadly screen uncovered genes. Figure S3 shows examples of modifiers identified by this latter approach. Although the nutrient sensing fat body and other tissues outside of the CNS play important roles in Drosophila

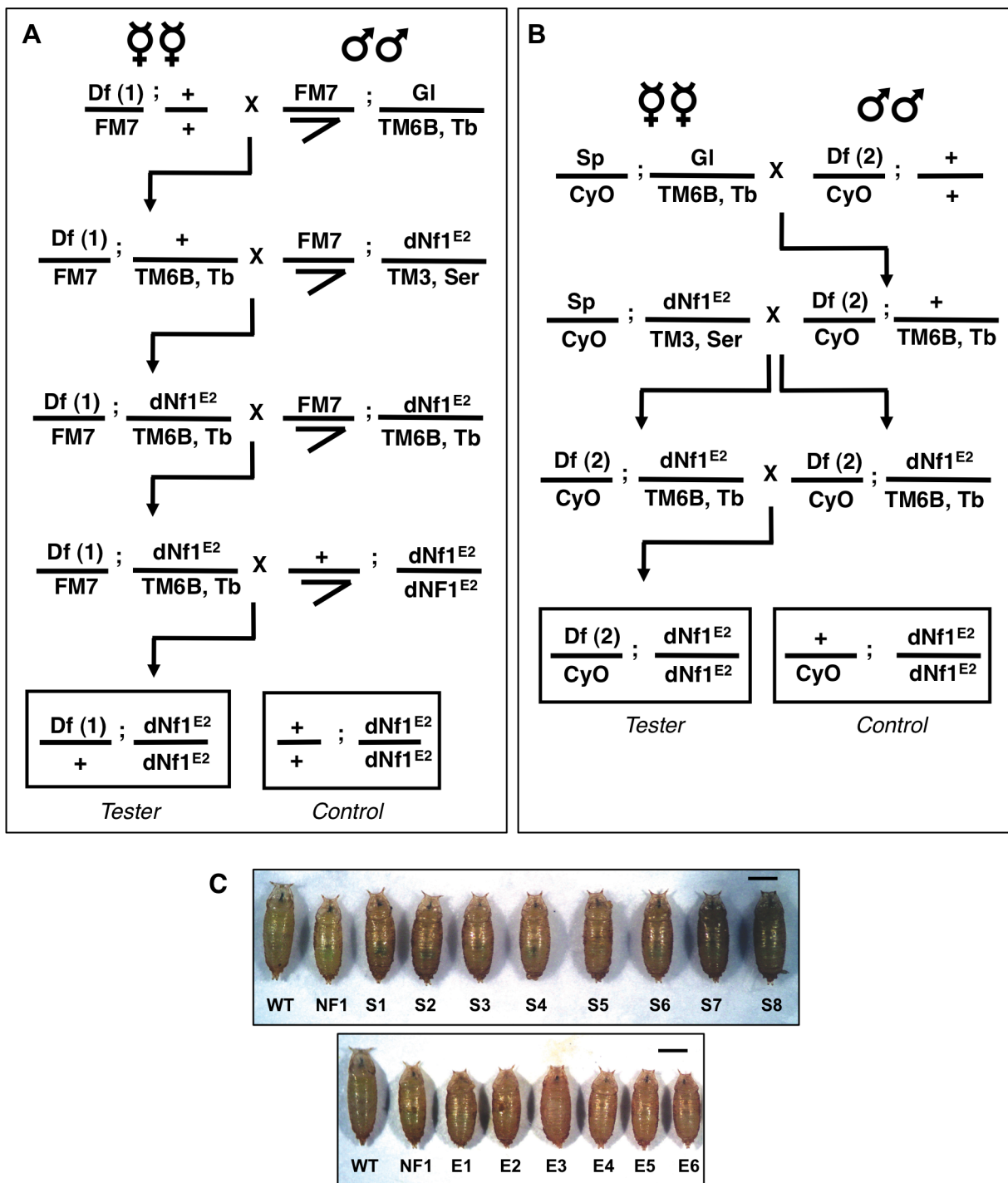


Figure 2. Deficiency screen for dominant modifiers of the *dNf1* growth defect. Isogenic 1st and 2nd chromosome deficiencies from the Exelixis, DrosDel and Bloomington Stock Center collections were tested for their ability to alter *dNf1* female pupal size. Crossing schemes to generate *Df(1)/+*; *dNf1^{E2}* (A) and *Df(2)/CyO; dNf1^{E2}* (B) screening stocks. The *tubby*-marked *TM6B* 3rd chromosome balancer allowed the selection of *dNf1^{E2}* homozygotes for measurements. (C) Examples of deficiencies that suppress or enhance the *dNf1* size defect. Scale bar = 1 mm.

growth control [33,34], candidate modifiers have only been tested by RNAi knockdown in neurons or glial cells. We focused on these cell types, because neuronal *UAS-dNf1* expression sufficed to suppress the growth phenotype [5].

The *dNf1* pupal size modifiers identified to date can be classified into three non-exclusive categories, the first of which consists of the

previously implicated *dAlk/jeb* receptor/ligand pair and two not previously implicated other genes involved in Ras-mediated signal transduction. Another expected category includes genes involved in cAMP/PKA signaling, including the previously reported *dnc* cAMP phosphodiesterase suppressor [35], and the newly identified PKA catalytic subunit gene, *PKA-CI*, which acts as an enhancer.

Table 1. Deficiency screen summary.

Chromosome	Number screened	% genes uncovered	dNf1 Modifiers		Non-specific modifiers		dNf1 modifying loci	
			SUP	ENH	SUP	ENH	SUP	ENH
1	139	82.1	48	2	5	2	30	2
2L	182	87.7	14	15	1	7	11	10
2R	165	86.9	31	2	4	1	22	1

Indicated are the number of chromosome 1, 2L and 2R deficiencies screened, the fraction of genes uncovered (based on the FB2013_03 FlyBase release), the number of dNf1 modifying deficiencies and loci identified, and the number of non-specific modifiers.

doi:10.1371/journal.pgen.1003958.t001

This group also includes the *CCKLR-17D1* drosulfakinin receptor, recently implicated as a cAMP-coupled promoter of synaptic growth [36], which is particularly interesting given the recent identification of a *dNf1* larval NMJ overgrowth phenotype [16]. Finally, our screen also identified multiple genes whose roles in *dNf1* growth control had not been anticipated and whose functional relevance remains to be established. Several genes in this group are predominantly expressed in brain or have known neuronal functions, including genes coding for the aforementioned CCKLR-17D1 receptor, the synaptic scaffold protein Dap160, the neuronal RNA binding protein elav, the neuronal Na,K ATPase interacting protein NKAIN [37], and the larval brain and alimentary channel expressed amino acid transporter NAAT1 [38]. Other genes in this group include *CKIIbeta2*, encoding a casein kinase regulatory subunit, the endosomal trafficking proteins *deep-orange* and *carnation*, the Notch modifier heparan sulfate 3-O sulfotransferase *Hs3st-B* [39], and the ubiquitin E3 ligases *HERC2*, which acts as a suppressor, and *CUL3*, which has the opposite effect. Table 2 lists deficiencies that modify *dNf1* but not wild-type pupal size, limited to those for which the responsible gene has been identified. Table S2 identifies all analyzed deficiencies, indicates which modified *dNf1* pupal size (providing female pupal sizes as a gauge of modification strength), which also altered wild-type pupal size, and which deficiencies altered developmental timing.

dNf1 Pupal Size Modifiers Involved in Jeb/dAlk/Ras/ERK Signaling

We previously reported that the *dAlk* receptor tyrosine kinase [40] acts as a rate-limiting activator of neuronal Ras/ERK pathways responsible for *dNf1* size and learning defects [15]. Therefore, the fact that the *dAlk* and *jeb* genes are uncovered by one and two suppressing deficiencies, respectively (Table 2), validates our screen. Others recently reported that Jeb/dAlk signaling allows brain growth to be spared at the expense of other tissues in nutrient restricted Drosophila, and identified a glial cell niche around neuroblasts as the source of Jeb under these conditions [41]. To determine whether glial cells also produce Jeb involved in overall growth control under normal conditions, we used glial and neuronal Gal4 drivers to test the effect of tissue-specific *jeb* and *dAlk* knockdown. Arguing that neurons are the main source of Jeb involved in systemic growth control under non-starvation conditions, *jeb* knockdown with the *Ras2-Gal4*, *C23-Gal4*, and *n-syb-Gal4* neuronal drivers [5] increased *dNf1*^{E2} pupal size (Figure 5A), whereas the *Nrv2-Gal4*, *Eaat1-Gal4* and *Gli-Gal4* glial drivers had no effect (data not shown). The only glial driver that gave rise to partial rescue was the pan-glial *repo-Gal4* line, although this effect was not enhanced by co-expressing *UAS-Dcr2*. Control experiments showed that any driver used in these and other experiments had no effect on pupal size in the absence of

UAS transgenes or vice-versa, that UAS transgenes had no effect in the absence of Gal4 drivers (Figure 5A and data not shown). Finally, extending previous findings and further confirming a role for *jeb* as a dominant *dNf1* size defect suppressor, the *jeb*^{wedl} loss-of-function allele [42] dominantly increased *dNf1* pupal size (Figure 5B)

Previously, heterozygous mutations affecting RAF/MEK/ERK kinase cascade components *Draf* (*pole hole*; *phl*), *Dsor1*/dMEK, or *ERK/rolled* (*rl*), did not modify *dNf1* size [5]. In agreement, two *phl*-uncovering deficiencies, *Df(1)ED6574* and *Df(1)ED11354*, did not score as modifiers (Table S2). No *rl* uncovering deficiencies were analyzed, but *Df(1)Exel9049*, which is among the stronger suppressors identified, deletes *Dsor1* and only two other genes, the neurogenic gene *almondex* (*amx*), and *CG17754*, predicting a BTB and Kelch domain protein. Arguing that reduced Ras/ERK signaling upon loss of *Dsor1* combined with abnormal neuronal differentiation due to loss of *amx* may synergistically cause the observed strong effect, *Ras2-Gal4* driven UAS-RNAi transgenes targeting either gene, while causing pupal lethality at 25°C, increased *dNf1* pupal size at lower temperatures (Figure 5C). Moreover, suppression of the *dNf1* pupal size defect was also observed upon individual heterozygous loss of either *Dsor1* or *amx*, although at least with the tested alleles, combined loss of both genes did not have a more pronounced effect (Figure 5B). Previously, we did not observe suppression of the *dNf1*^{E2} pupal size defect in crosses with the *Dsor1*^{S-1221} allele [5]. A potential explanation may be that *Dsor1*^{LH110} is a null mutant [43], whereas the molecular nature of *Dsor1*^{S-1221} is undetermined. Genetic background differences between these *Dsor1* alleles are another potential explanation for the discrepant results.

Multiple screens aimed at identifying genes involved in Drosophila tyrosine kinase/Ras signaling have been performed [44–52]. Among the genes identified, several are uncovered by 1st and 2nd chromosome deficiencies that do not modify *dNf1* size. Suppressing *Df(2R)BSC161* uncovers 27 genes including *connector enhancer of KSR* (*cnk*), a scaffold protein that functions as a bimodal (both positive and negative) regulator of RAS/MAPK signaling [53,54]. Supporting a role for *cnk* as a *dNf1* modifier, the *cnk*^{XE-383} and *cnk*^{E-2083} alleles acted as dominant suppressors (Figure 5B), and suppression was also observed upon RNAi-mediated *Cnk* knockdown using *Ras2-Gal4* or *P(GawB)C23-Gal4* neuronal drivers (Figure 5C). However, *Df(2R)BSC154*, which uncovers *cnk* and only nine other genes, did not score as a modifier (Table S2).

dNf1 Size Modifiers Involved in cAMP/PKA Signaling

The *dNf1* growth defect is suppressed by heat shock-induced expression of a constitutively active murine PKA catalytic subunit transgene, called PKA* [4], or by loss of the *dunce* (*dnc*) cAMP phosphodiesterase [35]. Further validating our screen, two *dnc* uncovering deficiencies and another that removes the region

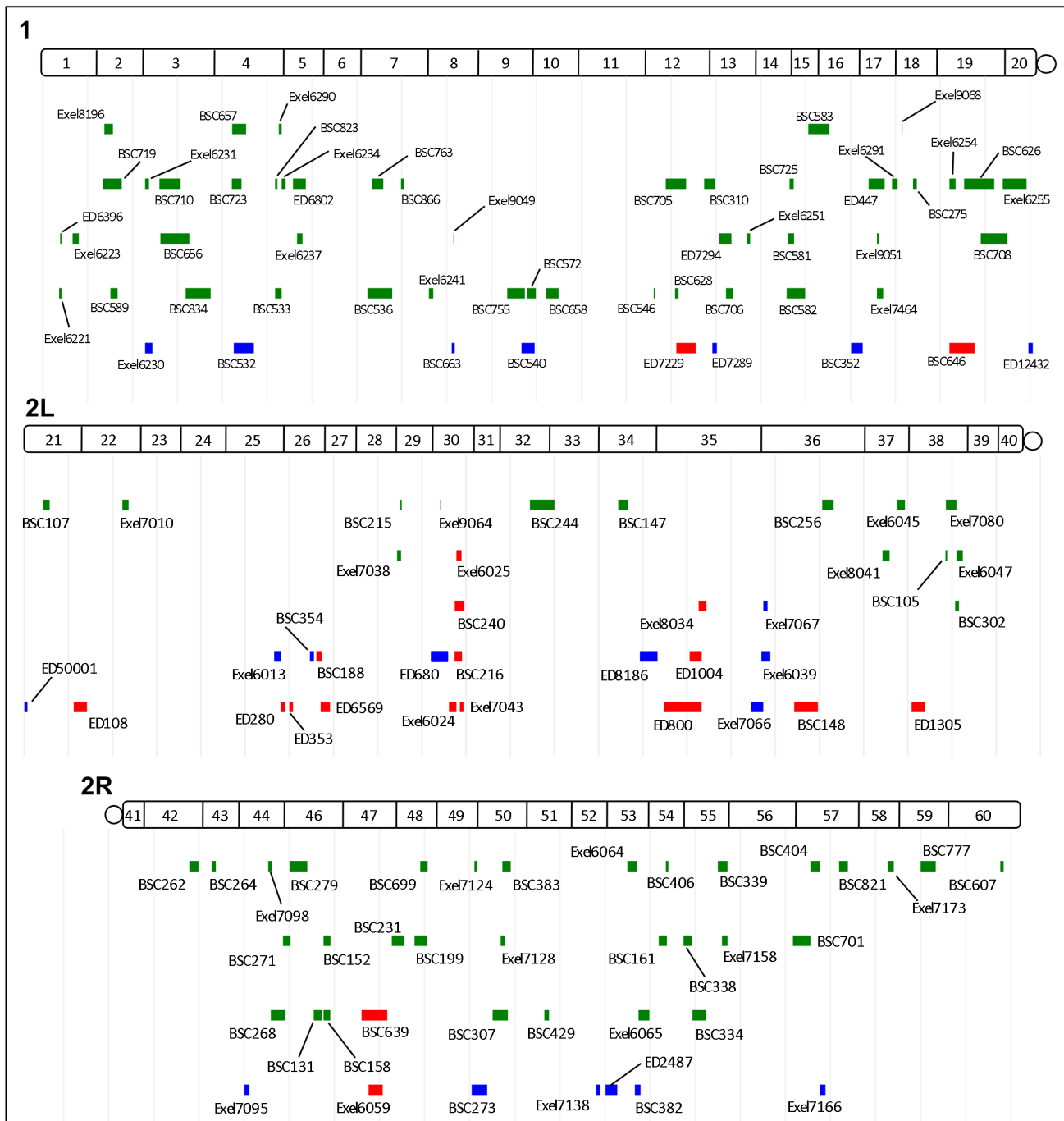


Figure 3. Cytogenetic locations of *dNf1* modifying deficiencies. Locations of modifying deficiencies (drawn to scale) on the 1st and 2nd (2L and 2R) chromosomes. Deficiencies that enhance or suppress are shown in red and green, respectively. Non-specific deficiencies that dominantly affect the size of wild-type pupae are in blue. Many modifying deficiencies uncover overlapping genomic segments.
doi:10.1371/journal.pgen.1003958.g003

immediately upstream of the *dnc* coding region, all scored as suppressors (Table 2). Moreover, the *Pka-R2* gene, encoding a cAMP binding regulatory PKA subunit, whose dissociation from the catalytic subunit activates the latter, is uncovered by two additional suppressing deficiencies, whereas a deficiency that uncovers the major *Pka-C1* catalytic subunit gene scored as an enhancer (Table 2). *Df(1)ED7261*, which uncovers the *rutabaga (rut)* adenylyl cyclase, did not score as a modifier (not shown). Confirmation of *dnc* and *Pka-C1* as the genes responsible for the

observed effects was obtained in crosses with three *dnc* and three *Pka-C1* loss-of-function alleles (Table 2). *Pka-R2* remains an attractive candidate suppressor, but expression *Pka-R2^{RNAi}* transgenes in neurons had no effect and its role as a *dNf1* modifier remains unconfirmed (results not shown).

Novel *dNf1* Modifiers

Recently, the cAMP-coupled CCKLR-17D1 drosulfakinin receptor, but not its closely related CCKLR-17D3 paralog, was

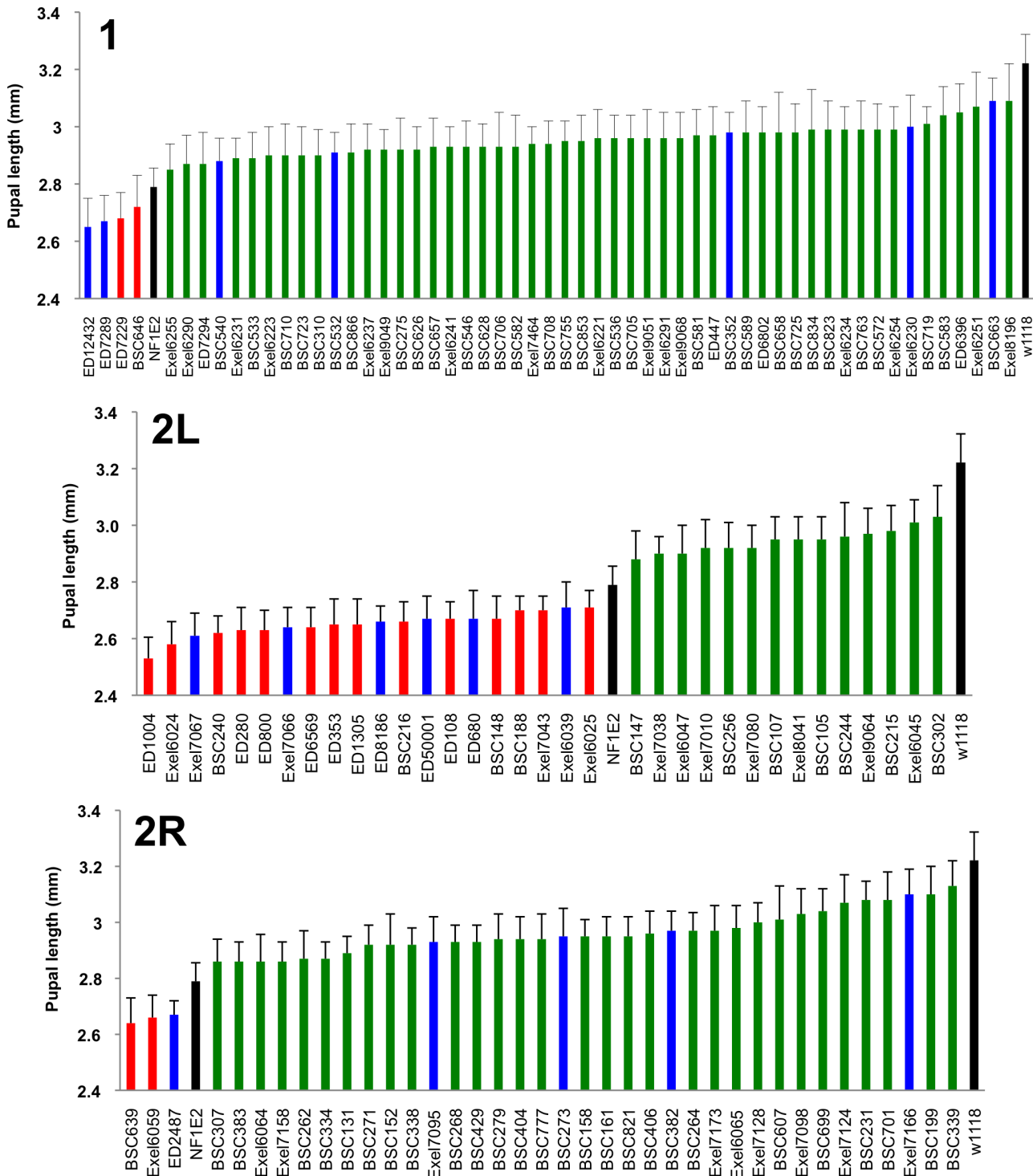


Figure 4. Identified deficiencies increase or decrease pupal size to different extents. Female pupal lengths for the indicated 1, 2L and 2R deficiencies. Control measurements for *dNf1*^{E2} and wild-type (*w*¹¹¹⁸) are in black. Colors for enhancing, suppressing and non-specific deficiencies are as in Figure 2. Pupal lengths are shown in mm, error bars denote standard deviations and are based on measurements described in Table S2. All shown deficiencies modify *dNf1* female pupal size with *p*-values < 0.01.
doi:10.1371/journal.pgen.1003958.g004

identified as a positive regulator of synaptic growth [36]. The *CCKLR-17D1* gene is uncovered by three suppressing deficiencies, including *Df(1)Exel9051*, which uncovers only three other genes. The closely linked *CCKLR-17D3* paralog is not uncovered by *Df(1)Exel9051*, and while *Ras2-Gal4* or *P(GawB)C23-Gal4* driven

neuronal *CCKLR-17D1* RNAi expression strongly suppressed the *dNf1* pupal size defect, similar suppression of *CCKLR-17D3* had no effect (Figure 6A).

Beyond *CCKLR-17D1*, several *dNf1* size modifiers are expressed in brain and/or have neuronal functions. Among these, dynamin-

Table 2. Modifying deficiencies and identification of responsible genes.

Deficiency	Cytological Breakpoints	Modif.	Gene Implicated	Modifying allele(s) and/or RNAi
Tyrosine Kinase/Ras signaling				
Df(2R)Exel7144	53C8;53D2	SUP	<i>dAlk</i>	<i>dAlk</i> ⁸ (lof), <i>dAlk</i> ⁹ (lof), v11446, v107083, JF02668
Df(2R)Exel6064	53C11;53D11			
Df(2R)BSC199	48C5;48E4	SUP	<i>Jellybelly (jeb)</i>	<i>Jeb</i> ^{weli} (lof), v103047, v30800
Df(2R)BSC699	48D7;48E6			
Df(2R)BSC161	54B2;54B17	SUP	<i>connector enhancer of ksr (cnk)</i>	<i>cnk</i> ^{XE-385} (Δ), <i>cnk</i> ^{E-2083} (lof), v107746
Df(1)BSC663	8D1;8D5	SUP	<i>Dsor1</i> and <i>almondex (amx)</i>	<i>Dsor1</i> : <i>Dsor1</i> ^{LH110} (amorph), v107276, v40026, HMS00145;
Df(1)Exel9049	8D2;8D3			amx: <i>amx</i> ⁰⁶³⁶² (hypo), v3296
cAMP/PKA signaling				
Df(1)BSC710	3B2;3C9	SUP	<i>dunce (dnc)</i>	<i>dnc</i> ^{M14} (amorph), <i>dnc</i> ^{ML} (amorph), <i>dnc</i> ¹ (hypo)
Df(1)BSC656	3B3;3D2			
Df(1)BSC834	3C11;3F3			
Df(2L)Exel6024	30C1;30C9	ENH	<i>cAMP-dependent protein kinase 1 (PKA-C1)</i>	<i>PKA-C1</i> ^{BG02142} (leth), <i>PKA-C1</i> ⁰⁶³⁵³ (hypo), <i>PKA-C1</i> ^{B3} (leth)
Neuronal Function				
Df(1)ED447	17C1;17F1	SUP	<i>CCK-like receptor at 17D1 (CCKLR-17D1)</i>	v100760
Df(1)Exel9051	17D1;17D3			
Df(1)Exel7464	17D1;17E1			
Df(2L)BSC302	39A1;39A6	SUP	<i>Dynamin-associated protein 160 (Dap160)</i>	<i>Dap160</i> ^{A1} (lof), <i>Dap160</i> ^{A2} (lof), v106689, v16158, JF01918
Df(2L)Exel6047	39A2;39B4			
Df(1)Exel6221	1B4;1B8	SUP	<i>Embryonic lethal abnormal vision (elav)</i>	<i>elav</i> ^{G0031} , <i>elav</i> ¹
Df(1)ED6396	1B5;1B8			
Df(2L)BSC216	30C6;30E1	ENH	<i>Nicotinic Acetylcholine Receptor alpha-30D (nAcRα-30D)</i>	<i>nAcRα-30D</i> ^{DAS1} (via) <i>nAcRα-30D</i> ^{DAS2} (via) <i>nAcRα-30D</i> ^{KG0582} (via)
Df(2L)BSC240	30C7;30F2			
Df(2L)Exel7043	30D1;30F1			
Df(2L)Exel6025	30C9;30E1			
Df(2L)Exel8041	37D7;37F2	SUP	<i>Rab9</i>	v107192, v36200, HMS02635
Other				
Df(1)Exel6254	19C4;19D1	SUP	<i>HERC2</i>	v105374
Df(2L)ED800	35B2;35D1	ENH	<i>Cullin-3 (cul3)</i>	<i>cul3</i> ^{gft2} (lof)
Df(2L)ED1050	35B8;35D4			
Df(2L)ED1004	35B10;35D1			
Df(1)BSC533	4F4;4F10	SUP	<i>Neutral amino acid transporter 1 (NAAT1)</i>	v106027, v37380, v50063
Df(1)Exel6290	4F7;4F10			
Df(1)Exel9068	18B4;18B6	SUP	<i>Heparin sulfate 3-O sulfotransferase-B (Hs3st-B)</i>	v110601
Df(2R)BSC701	56F15;57A9	SUP	<i>Casein kinase II β2 subunit (CKIIβ2)</i>	v102633, v26915
Df(2R)BSC607	60E4;60E8	SUP	<i>Na,K-ATPase Interacting (NKAIN)</i>	v105893, v102018
Df(1)BSC275	18C8;18D3	SUP	<i>Vps33/carnation (car)</i>	<i>car</i> ¹ (hypo), <i>car</i> ^{Δ146} (lof), v110756
Df(1)BSC719	2A3;2B13	SUP	<i>Vps18/deep orange (dor)</i>	<i>dor</i> ⁸ (leth), v107053, v105330
Df(1)Exel8196	2B1;2B5			
Df(1)BSC589	2B3;2B9			

Modifying deficiencies for which the responsible *dNf1* interacting gene has been identified. The cytological location, and the dominant effect on *dNf1* pupal size (SUP – suppressor, ENH – enhancer) of each deficiency is given. The responsible genes for each modifying deficiency are shown with the mutant alleles, VDRC and TRIP RNAi lines used in their identification. Expression of RNAi transgenes was induced with the *Ras2-Gal4*, *elav-Gal4*, *n-syb-Gal4* and/or *C23-Gal4* drivers. Abbreviations: hypo: hypomorphic; leth: lethal; lof: loss-of-function; amorph: amorphic; Δ : deletion; via: viable.

doi:10.1371/journal.pgen.1003958.t002

associated protein 160 (Dap160) is an intersectin-related scaffold implicated in synaptic vesicle exocytosis and neuroblast proliferation [55–58]. *Dap160* is uncovered by suppressing deficiencies *Df(2L)Exel6047* and *Df(2L)BSC302*, whose region of overlap encompasses ten genes. We note that *Df(2L)Exel6047* also uncovers the Drosophila *Ret* tyrosine kinase gene, the human ortholog of which is the receptor for glial-derived neurotrophic factor. *Ret* initially appeared an especially attractive candidate

suppressor, because activating *RET* and inactivating *NF1* mutations can both lead to human pheochromocytoma [59], and because Drosophila *Ret* is expressed in larval brain neurons that resemble neuroendocrine cells [60]. However, among multiple lines of evidence that argue against a role for *Ret* in the *dNf1* growth defect, *UAS-dNf1* re-expression directed by a newly generated *Ret-Gal4* driver that recapitulates the endogenous larval brain *Ret* expression pattern (Figure S4B), or

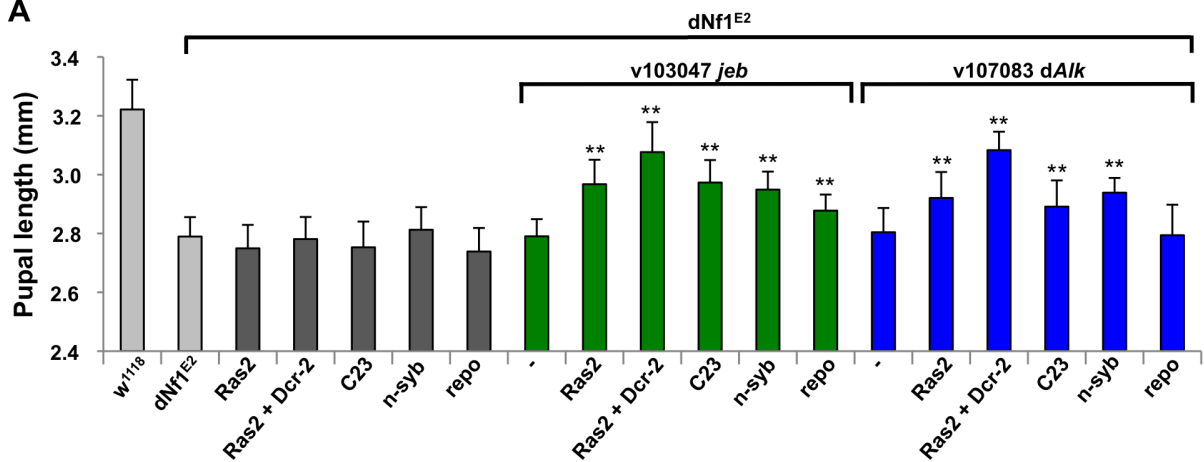
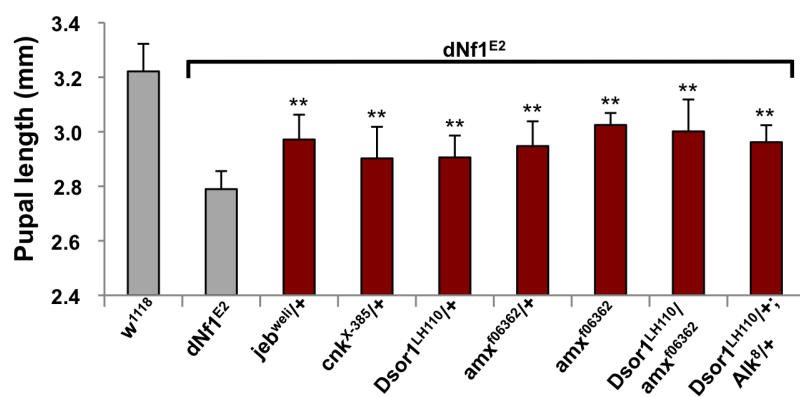
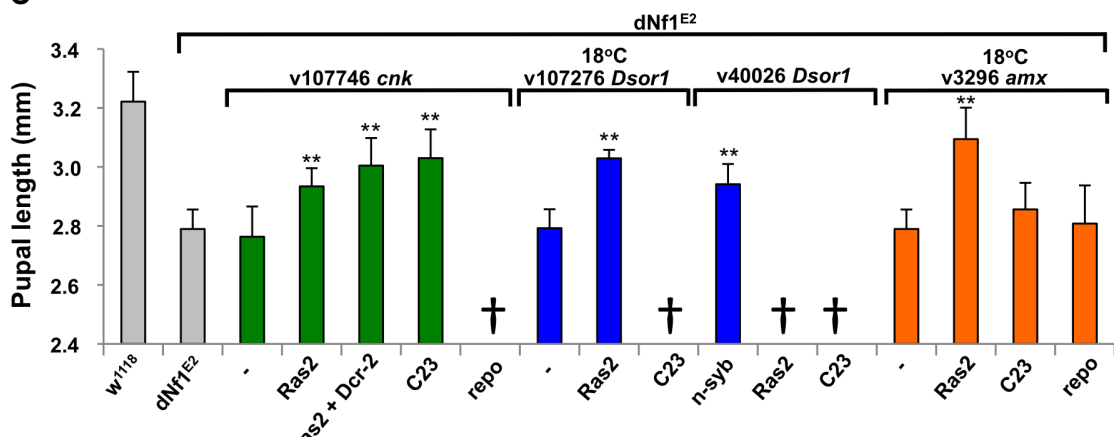
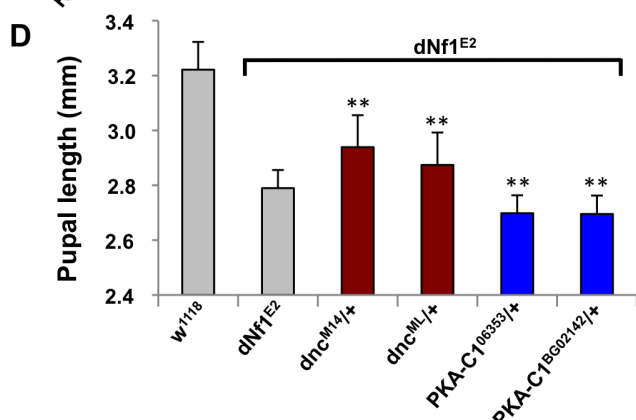
A**B****C****D**

Figure 5. Validation of *dNf1* modifiers involved in Jeb/dAlk/Ras/ERK and cAMP signaling. (A) Neuronal expression of *dAlk* RNAi using *Ras2-Gal4*, *Ras2-Gal4+UAS-Dcr-2*, *c23-Gal4* or *n-syb-Gal4* drivers suppresses the *dNf1* size defect. Expression of *jeb* RNAi with the same neuronal drivers also suppresses. Weaker suppression is observed when *jeb* RNAi expression is controlled by the pan-glial *repo-Gal4* driver. Dark grey bars are control measurements of Gal4 drivers in the *dNf1* background. Light grey bars are sizes of wild-type (w^{1118}) and *dNf1^{E2}* controls. (B) Suppression of the *dNf1* size defect by the indicated *jeb*, *cnk*, *Dsor1* and *amx* alleles. (C) Neuronal *cnk*, *Dsor1* or *amx* knockdown suppressed the *dNf1* size defect. In the case of *Dsor1 v107276* and *amx*, cultures were maintained at 18°C to prevent lethality observed at 25°C. Some RNAi transgene/driver combinations were lethal (†) even at 18°C. (D) Validation of *dnc* and *Pka-C1* as *dNf1* modifiers was obtained in crosses with *dnc^{M14}*, *dnc^{ML}*, *Pka-C1⁶³⁵³* and *Pka-C1^{BG02142}* loss-of-function alleles. In this and subsequent figures, * and ** denote p-values < 0.05 and < 0.01, respectively.

doi:10.1371/journal.pgen.1003958.g005

RNAi-mediated *Ret* inhibition, did not modify *dNf1* pupal size, nor did expression of a *UAS-Ret* K805A kinase dead transgene. Moreover, *Ret-Gal4* driven expression of *UAS-Ret* transgenes carrying the activating C695R mutation, which mimics a mutation found in multiple endocrine neoplasia type 2 did not phenocopy the *dNf1* reduced growth phenotype, although the same transgene did produce the previously described rough eye phenotype when driven by *GMR-Gal4* [60]; Figure S4C]. Further arguing against a role in *dNf1* growth control, *Ret* is uncovered by non-modifying *Df(2L)BSC312*. By contrast, *Dap160* loss-of-function alleles (*Dap160^{A1}* and *Dap160^{A2}*; [56]), or *Dap160* RNAi expression driven by three neuronal Gal4 drivers, suppressed the *dNf1* pupal size defect, identifying it as the responsible modifier (Figure 6B).

The gene for the neuronal RNA binding protein *elav* is uncovered by suppressing *Df(1)Exel6221* and *Df(1)ED6396* whose region of overlap includes just three other genes. Identifying *elav* as the responsible modifier, *elav¹* and *elav^{G0031}* alleles strongly suppressed (Figure 6C). *Rab9* is a modifier uncovered by suppressing deficiency *Df(2L)Exel8041*. Neuronal but not glial *Rab9^{RNAi}* expression increases

dNf1 pupal size, and the same result is seen upon neuronal expression of a *Rab9* dominant negative [61] mutant (Figure 6D).

NAAT1, coding for a larval gut and brain expressed amino acid transporter with a unique affinity for D-amino acids [38], is uncovered by suppressing *Df(1)Exel6290* and *Df(1)BSC533* whose region of overlap includes only four other genes. Identifying *NAAT1* as the responsible suppressor, three neuronal Gal4 lines driving the expression of three *NAAT1* targeting RNAi transgenes suppressed the *dNf1* size defect, whereas *Repo-Gal4* driven glial expression had no effect (Figure 7A and Table 2).

Mammalian E3 ubiquitin ligase *HERC2* controls the ubiquitin-dependent assembly of DNA repair proteins on damaged chromosomes [62]. Drosophila *HERC2* is uncovered by suppressing deficiency *Df(1)Exel6254*, which also uncovers the *syx16*, coding for syntaxin 16. No *HERC2* alleles exist, but *Ras2-Gal4* driven expression of a *UAS-HERC2^{RNAi}* transgene (*v105374*) strongly suppressed the *dNf1* pupal size defect (Figure 7A), whereas similar knockdown of *Syx16* had no statistically significant effect (not shown). The gene for another E3 ligase component, *Cul-3*, is

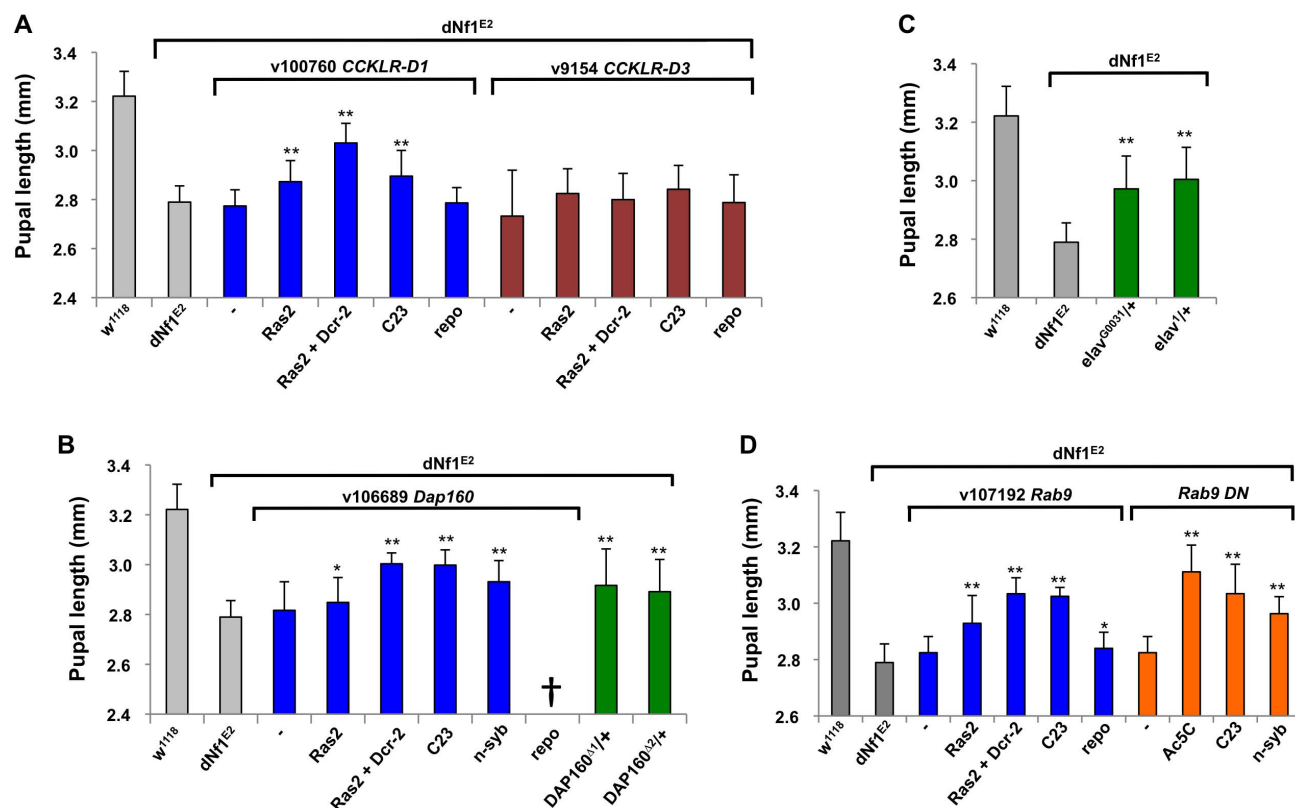


Figure 6. Validation of *dNf1* modifiers with neuronal functions. (A) *Ras2-Gal4* or *C23-Gal4* driven neuronal RNAi knockdown of *CCKLR-17D1* but not *CCKLR-17D3* suppressed the *dNf1* pupal size defect. (B) Identification of dynamin-associated protein 160 (Dap160) as a suppressor of *dNf1* growth. Neuronal RNAi targeting of *Dap160* increased *dNf1* pupal size as did two *Dap160* loss-of-function alleles. (C) Two *elav* alleles dominantly suppress the *dNf1* size defect. (D) Neuronal expression of a *Rab9* RNAi transgene or of a dominant negative *Rab9* mutant suppresses the *dNf1* size defect.

doi:10.1371/journal.pgen.1003958.g006

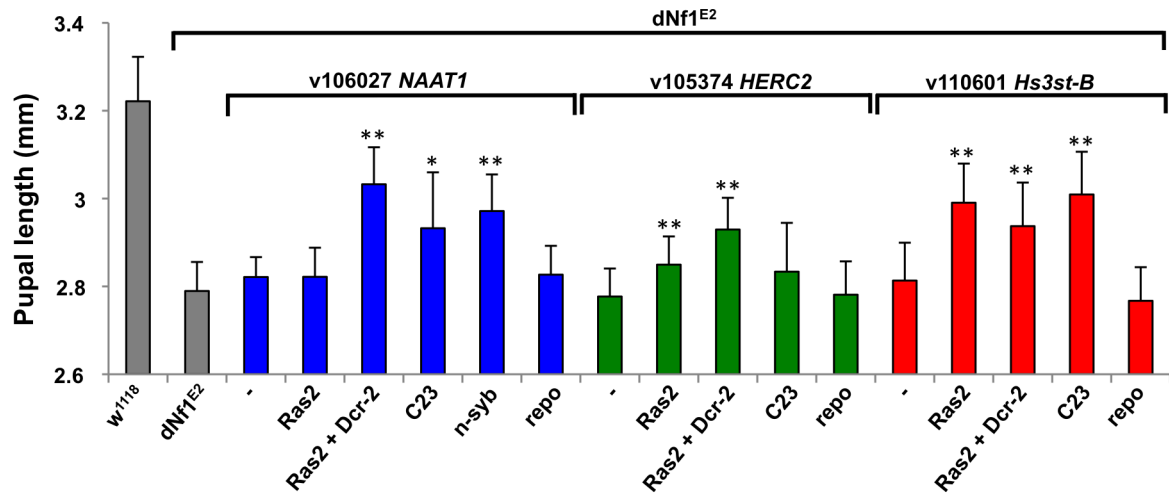
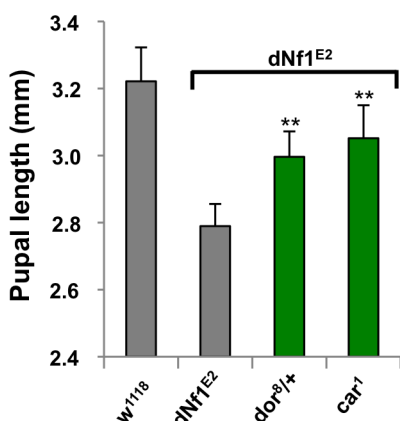
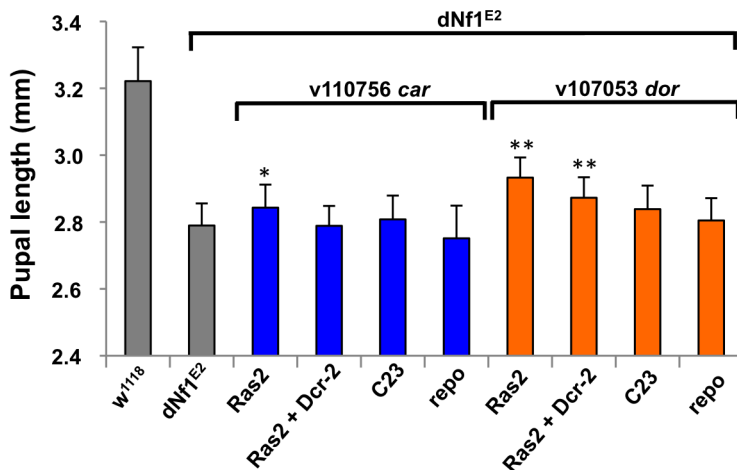
A**B****C**

Figure 7. Identification of modifying genes with undetermined roles in *dNf1* suppression. (A) Validation of *NAAT1*, *HERC2* and *Hs3st-B* as *dNf1* modifiers. All three genes were identified by systematic RNAi screening of genes uncovered by suppressing deficiencies. (B) Loss-of-function alleles of Class C Vacuolar Protein Sorting complex subunits *carnation* (*car/Vps33A*) and *deep-orange* (*dor/Vps18*) increase *dNf1* pupal size. (C) RNAi-mediated neuronal *car* or *dor* knockdown was not particularly effective, suggesting these genes may function elsewhere to modify *dNf1*-dependent growth.

doi:10.1371/journal.pgen.1003958.g007

uncovered by three enhancing deficiencies, and a *Cul-3* loss-of-function allele or *Ras2-Gal4* driven expression of a *Cul-3* RNAi transgene both enhanced the *dNf1* size defect, identifying it as the responsible gene (Table 2).

Suppressing *Df(1)Exel9068* uncovers only four genes, including one encoding the TORC2 complex subunit Rictor. However, systematic *Ras2-Gal4* driven RNAi knockdown of *Df(1)Exel9068* uncovered genes identified *Hs3st-B*, encoding one of two Drosophila heparan sulfate 3-O sulfotransferases, as a potent *dNf1* size defect suppressor (Figure 7A), whereas knockdown of Rictor had no effect (not shown). Others previously identified *Hs3st-B* as a positive regulator of Notch signaling [39]. However, the heparan sulfate proteoglycan substrates of *Hs3st-B* bind various growth factors and other ligands and have been implicated in a variety of biological processes. Exactly why loss of *Hs3st-B* suppresses the *dNf1* growth defect remains to be determined.

Two functionally related *dNf1* growth defect suppressors *carnation* (*car/Vps33A*) and *deep-orange* (*dor/Vps18*), encode subunits

of the Class C Vacuolar Protein Sorting (VPS) complex, required for the delivery of endosomal vesicles to lysosomes [63]; Figure 7B]. The *Vps16A* gene encodes a third member of this complex [64], but whether *Vps16A* located on the 3rd chromosome also acts as a *dNf1* suppressor, or whether pharmacological inhibition of lysosomal degradation affects *dNf1* pupal size are questions that remain to be answered.

B4/Susi is a coiled-coil protein without obvious orthologs outside of insects. It functions as a negative regulator of Drosophila class I phosphatidylinositol-3 kinase Pi3K92E/Dp110 by binding to its Pi3K21B/dP60 regulatory subunit. Homozygous *B4* mutants have an increased body size [65], which may explain why *Ras2-Gal4*-driven RNAi-mediated suppression of *B4*, uncovered by suppressing deficiency *Df(2L)BSC147*, increased *dNf1* pupal size (not shown). However, whether *B4* is the responsible dominant modifier is doubtful, given that it is also uncovered by *Df(2L)BSC692*, a non-modifying deficiency. Moreover, we previously found that heterozygous loss of *Pi3K21B*, or neuronal

expression of a dominant negative *Pi3K92E* transgene, did not modify *dNf1* pupal size [5]. Beyond *B4*, *dNf1* size modifying deficiencies uncovered no genes involved in the canonical growth regulating pathways mediated by insulin and ecdysone. Indeed, several such genes were uncovered by non-modifying deficiencies. Among these genes, fat body expressed insulin-like growth factor *Iip6*, which regulates larval growth in the post-feeding phase [66,67], is uncovered by two non-modifying deficiencies. A single non-modifying deficiency, *Df(2L)BSC206*, uncovers both the *chico* and *pten* genes, whose products antagonistically control insulin-stimulated Pi3K92E/Dp110 activity, leading to changes in body, organ, and cell size [68,69]. Among subunits of the cell growth regulating mTORC1 complex, *raptor* is uncovered by three and *Tor* by one non-modifying deficiency. Among genes implicated in ecdysone signaling, the ecdysone co-receptor *ultraspire* and the ecdysone-induced growth regulating *DHR4* nuclear receptor [70] are each uncovered by non-modifying deficiencies, and two such deficiencies uncover *Pth*, coding for prothoracotrophic hormone, which provides developmental timing cues by stimulating the production of ecdysone [71,72]. These results reinforce our conclusion that the canonical growth regulating pathways involving insulin and ecdysone play no obvious roles in *dNf1* growth control.

Manipulating cAMP/PKA Signaling in the Ring Gland Affects *dNf1* Systemic Growth Non-Cell-Autonomously

Several results argue that defects in Ras/ERK and cAMP/PKA signaling responsible for the *dNf1* growth defect involve non-overlapping cell populations. Firstly, heat shock-induced *hsp70-PKA**, or *Ras2-Gal4* induced attenuated *UAS-PKA** transgene (see below) expression rescued the *dNf1* pupal size defect, but failed to reduce the elevated larval brain phospho-ERK level (Figure 8A). Moreover, several neuronal RNAi drivers that increase *dNf1* pupal size when driving *UAS-dNf1* [5], failed to modify this phenotype when driving *dnc^{RNAi}* transgenes, even in the presence of the *UAS-Dcr-2* RNAi enhancer (Table 3). This prompted us to investigate whether genetic manipulation of cAMP/PKA signaling in cells other than *dNf1* requiring neurons was more effective.

To manipulate cAMP/PKA signaling tissue-specifically we used three *UAS-dnc^{RNAi}* transgenes. We also generated a series of attenuated *UAS-PKA** transgenes using vectors with modified Gal4-inducible promoters harboring just 2, 3 or 4 Gal4-binding UAS elements (Figure 8B and C). We made the latter transgenes because a *UAS-PKA** expression using the five UAS element containing standard UAS-T vector is lethal in combination with most Gal4 drivers [73]. As reported previously [74], driving *UAS-dNf1* ubiquitously with *Act5C-Gal4*, or broadly in neurons with *elav-Gal4*, *Ras2-Gal4*, *c23-Gal4*, or *386Y-Gal4* restored *dNf1* pupal size, whereas driving the same transgene with more restricted neuronal or non-neuronal drivers had no effect (Figure 8D and Table 3). By contrast, driving the expression of *UAS-dnc^{RNAi}* or attenuated *UAS-PKA** transgenes with the same set of broadly expressed neuronal drivers was ineffective (Tables 3 and S5). We note that expression of the 2×*UAS-PKA** and 3×*UAS-PKA** transgenes was generally well tolerated, whereas the 4×*UAS-PKA** and the 5×*UAS-PKA** transgenes exhibited increasing levels of lethality (Tables 3 and S5). Arguing that rescue of the *dNf1* growth defect by manipulating cAMP/PKA signaling or *dNf1* expression involves different cells, strong pupal size rescue was observed by increasing cAMP/PKA signaling in adipokinetic hormone-producing cells at the base of the neuroendocrine ring gland using the *Akh-Gal4* driver (Figure 8D). Rescue was also observed with the *Feb36-Gal4* and *Aug21-Gal4* ring gland drivers (Figure 8D), which give rise to expression in the corpora allata, the source of juvenile hormone,

but not with the *P0206-Gal4* or *Mai60-Gal4* drivers, which express predominantly in the prothoracic gland (Table 3). The tissue specificity of all Gal4 drivers used in this and other experiments was verified by microscopic observation of dissected *UAS-GFP* expressing larvae (Table S4 and Figures 8E–H and S5).

dAlk, *Jeb*, *Cnk* and *CCKLR-17D1* Suppress a *dNf1* NMJ Architectural Defect

During larval development, significant expansion of the NMJ arbor must occur, reflecting the steady muscle growth that takes place during larval life. As the NMJ grows, additional branches and boutons are added to the initial synaptic arbor that forms during late embryonic stages upon motor axon contact with its target muscle. As a result, at the wandering third instar stage, wild-type NMJs contain a highly stereotyped, segment specific number of synaptic boutons [75]. Recently, it was reported that *dNf1* functions presynaptically to constrain NMJ synaptic growth and neurotransmission [16]. In *dNf1* null mutant wandering third instar larvae, while the distribution of major presynaptic proteins is unaffected, increased overall size and synaptic bouton number is apparent at multiple NMJs, supporting a specific role for *dNf1* in restricting NMJ expansion [16]. Several *dNf1* suppressors that emerged in the current screen have also been linked to synapse morphogenesis, including *CCKLR-17D1*, which functions as a promoter of NMJ growth [36]. As our screen identified *CCKLR-17D1* as a dominant *dNf1* size defect suppressor, we wanted to confirm the *dNf1* NMJ phenotype and test whether *CCKLR-17D1* and other suppressors affected this defect.

By quantifying bouton number at the NMJ on muscles 6 and 7, we confirmed that *dNf1* mutants have a significant increase in mean bouton number (Figure 9A and B). In addition, this analysis confirmed previously published phenotypes for *dAlk*, *jeb* and *CCKLR-17D1* [36,76]. Importantly, the *dNf1* synaptic overgrowth phenotype is dominantly suppressed by *CCKLR-17D1*, *dAlk*, *jeb*, and *cnk* alleles (Figure 9B), arguing that all four genes are epistatic to *dNf1*. As a control we analyzed an allele of *spitz* (*spi*), which encodes an EGF-like growth factor and is uncovered by suppressing *Df(2L)Exel8041*. However, *spi* shows no genetic interaction with *dNf1*, as loss of *spi* modified neither the pupal size nor the NMJ overgrowth phenotypes (Figure 9B and data not shown).

Human ALK Is Expressed in Schwann Cells and May Serve as a Therapeutic Target in NF1

The identification of *dAlk* as a suppressor of all hitherto analyzed *dNf1* defects prompted us to explore whether human ALK represents a therapeutic target in NF1. Given our hypothesis that NF1 negatively regulates ALK stimulated Ras/ERK signaling, in order to play such a role, ALK and NF1 must be co-expressed in cells that give rise to symptoms. We previously found that *dNf1* and *dAlk* expression overlaps extensively in Drosophila larval and adult CNS [15], and the expression of orthologs of both genes also overlaps in the murine CNS [77,78]. While overlapping CNS expression is compatible with a role for ALK in NF1-associated cognitive dysfunction, a causative role in another hallmark NF1 symptom, peripheral nerve-associated tumors, is less obvious. Among the near universal symptoms on NF1, benign neurofibromas consist of Schwann cells, perineurial fibroblasts, infiltrating mast cells, and nerve elements, with the Schwann cells sustaining the second *NF1* hit [79]. To test whether increased ALK signaling in the absence of NF1 might play a role in the development of neurofibromas, we used reverse transcription/PCR to detect the

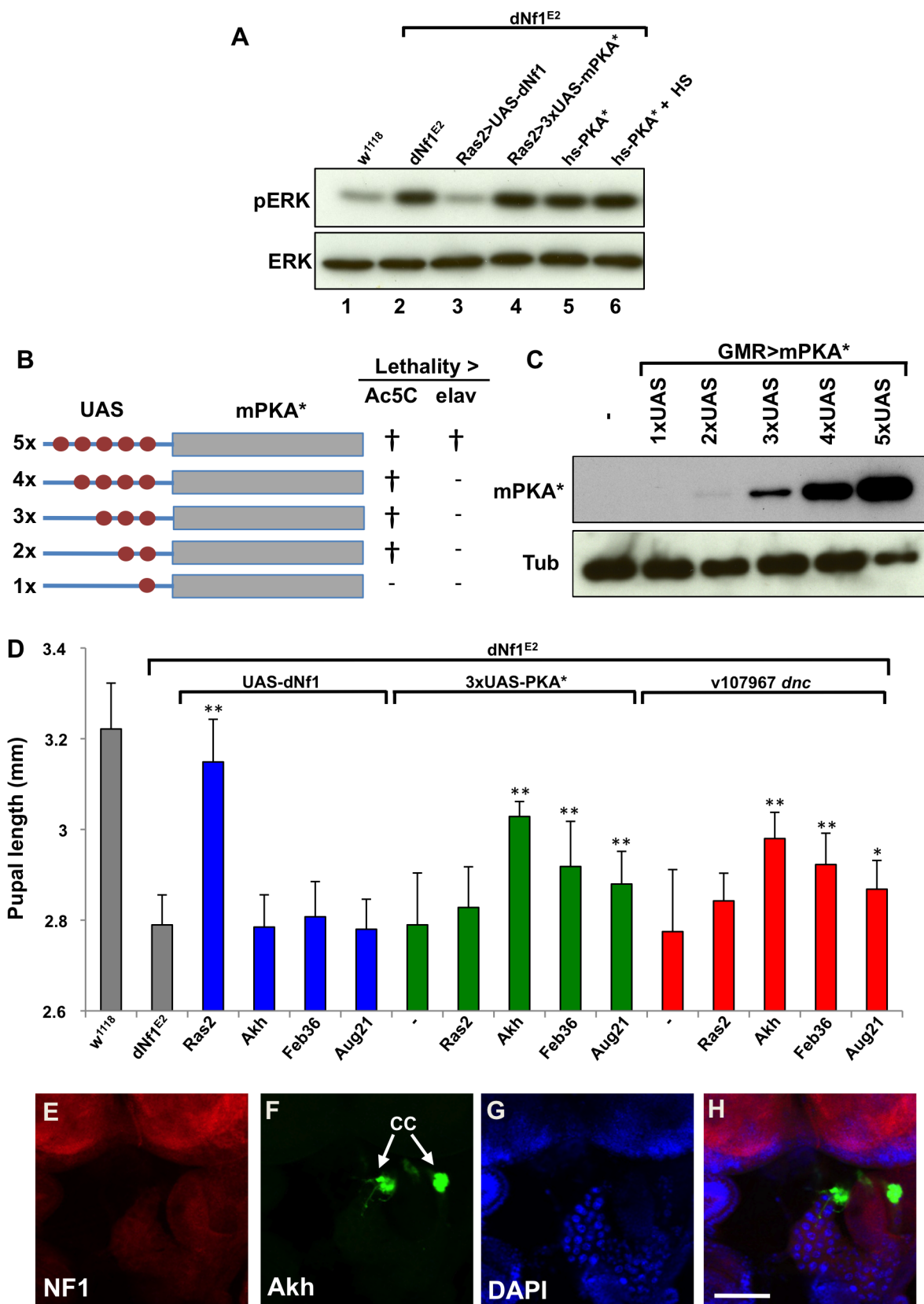


Figure 8. *dNf1* systemic growth related RAS/ERK and cAMP/PKA signals appear functionally and topographically distinct. (A) The elevated larval CNS pERK level of *dNf1* mutants is reduced by neuronal expression of *dNf1*, but not by neuronal or heat-shock induced ubiquitous expression of PKA*. Western blot of pERK levels in larval CNS of the indicated genotypes. In lane 6, larvae received a daily 20 min 37°C heat shock throughout development, a protocol that suppresses the *dNf1* growth defect [4]. (B) Structure of UAS-PKA* transgenes with 1 to 5 UAS elements. The

lethality of these transgenes when driven with either *Ac5C-Gal4* or *elav-Gal4* is indicated by † whereas (–) indicates viable offspring. (C) Western blot of adult head lysates showing relative expression of *GMR-Gal4*-driven transgenic PKA*. Tubulin is used as a loading control. (D) Expression of PKA* or knockdown of *dnc* by shRNAi in the ring gland rescues the *dNf1* pupal size defect. In contrast, *UAS-dNf1* expression with the same ring gland drivers fails to restore systemic growth. (E–H) Expression pattern of *Akh-Gal4* driving *UAS-GFP*, co-stained with DAPI and anti-dNf1. GFP expression in the corpora cardiaca (CC) is indicated. Scale bar = 50 μm. As previously noted [74], anti-dNf1 staining is strong in the CNS, whereas staining in the ring gland is close to background.

doi:10.1371/journal.pgen.1003958.g008

presence or absence of *ALK* mRNA in neurofibroma-derived *NF1*^{−/−} Schwann cells and *NF1*^{+/−} fibroblasts, using RNAs kindly provided by Drs. Eric Legius and Eline Beert. In these experiments, two different primer sets readily detected *ALK* mRNA in *NF1*^{−/−} Schwann cells, but not in *NF1*^{+/−} fibroblasts derived from the same tumors (Figure S6).

To test whether functional interactions between NF1 and ALK exist in human cells, we used the SK-SY5Y and Kelly neuroblastoma cells, both of which harbor constitutively active F1174L *ALK* alleles, and both of which are highly sensitive to pharmacological ALK inhibition [80]. Compatible with a role for NF1 as a negative regulator of mitogenic ALK/RAS signals, qRT-PCR verified *NF1* knockdown with two shRNA retroviral vectors increased the resistance of both lines to ALK inhibitors NVP-TAE684 and Crizotinib (Figures 10A, 10C and S7). Compatible with a model in which NF1 negatively regulates ALK/RAS signaling, *NF1* knockdown resulted in elevated ERK and AKT activation (Figures 10B). Moreover, expression of activated *KRAS*, *BRAF*, or *MEK* transgenes, but not of other Ras effector transgenes, in SH-SY5Y cells conferred similar resistance to ALK inhibition (Figure S8).

Discussion

The work reported here was motivated by the fact that human NF1 is a characteristically variable disease, the severity of which is controlled at least in part by symptom-specific modifier genes [81]. Thus, a genetic analysis in Drosophila might not only reveal molecular pathways controlled by the highly conserved (50% identical) dNf1 protein, but also provide clues to the identity of human modifiers, which by virtue of their rate-limiting roles in symptom development might serve as therapeutic targets. The current work was also motivated by the fact that, for reasons that remain poorly understood, most *dNf1* null mutant phenotypes are rescued by increasing, or phenocopied by decreasing, cAMP/PKA

signaling. The identification of genetic modifiers of a cAMP/PKA sensitive defect might reveal how loss of dNf1 affects cAMP/PKA signaling, and help to resolve the long-standing controversy as to whether dNf1 affects cAMP/PKA signaling directly, independent of its role as a Ras regulator [10,27], or indirectly, secondary to a Ras signaling defect [5,15].

While recognizing that none of the thus far identified *dNf1* phenotypes are ideally suited for use in modifier screens, we selected the pupal size defect as the phenotype to analyze in our screen for three main reasons. First, pupariation occurs at the end of the larval growth period, and pupal size is readily assessed by inspecting pupae attached to the side of culture vials, making this phenotype amenable to a large-scale screen. Second, the growth defect is among several cAMP/PKA sensitive *dNf1* phenotypes. Finally, reduced growth is also a symptom of human NF1 and other RASopathies [1,82]. However, while compelling reasons support the selection of this phenotype, confounding factors include that Drosophila size is a sexually dimorphic phenotype affected by population density, feeding, environmental conditions such as temperature, and genetic background differences. Moreover, while heterozygous *dNf1* mutants are marginally smaller than wild-type pupae [5], the more robust size phenotype (~15% reduction in linear dimensions, ~25% reduction in weight) used in our screen is only observed upon homozygous loss of *dNf1*. Thus, our screen was not designed to find modifiers that act on the dNf1 protein itself, like the recently identified SPRED proteins [83]. Finally, organism size is a function of growth rate and duration, both of which are regulated by hormonal cascades that involve cross-talk between the larval brain, the neuroendocrine ring gland, the fat body and other tissues [19,84]. Thus, a screen for modifiers of *dNf1*-regulated growth may uncover genes involved in various aspects of systemic growth control.

Early attempts to identify *dNf1* pupal size modifiers were abandoned when >95% of large X-ray induced 2nd chromosome

Table 3. Restoration of systemic growth by *dNf1* and cAMP/PKA involves different tissues.

Gal4	UAS-dNf1	<i>dnc v107967</i>	2×UAS-PKA*	3×UAS-PKA*	4×UAS-PKA*	5×UAS-PKA*
<i>Act5C</i>	Rescue	Rescue (pupal †)	SV	†	†	†
<i>elav</i>	Rescue	NR	NR	NR	NR	†
<i>elav+Dcr-2</i>	Rescue	NR	n/a	n/a	n/a	n/a
<i>Ras2(41)</i>	Rescue	NR	NR	NR	†	†
<i>Ras2(41)+Dcr-2</i>	Rescue	NR	n/a	n/a	n/a	n/a
<i>C23</i>	Rescue	NR	NR	NR	NR (pupal †)	†
<i>Feb36</i>	NR	Rescue	NR	Rescue	†	†
<i>Aug21</i>	NR	Rescue	Rescue	Rescue	Rescue	†
<i>Akh</i>	NR	Rescue	Rescue	Rescue	Rescue	Rescue (SV)

Act5C-Gal4 driven ubiquitous *dNf1* re-expression, or *elav-Gal4* and *Ras2-Gal4* driven neuronal re-expression rescues the *dNf1* pupal size defect, whereas *dnc* RNAi or UAS-PKA* expression controlled by the same drivers is ineffective. By contrast, expressing *dNf1* in specific parts of the neuroendocrine ring gland with the *Akh-Gal4*, *Feb36-Gal4* or *Aug21-Gal4* drivers fails to rescue, whereas using the same drivers to express *dnc* RNAi or attenuated UAS-PKA* transgenes does increase *dNf1* pupal size. All crosses produced viable adults unless otherwise indicated.

*denotes lethality, SV sub-viable, n/a not applicable, NR non-rescue.

The data shown summarize results of a larger effort to identify the tissues in which *dNf1* and cAMP/PKA affect systemic growth. Full results are shown in Table S5.
doi:10.1371/journal.pgen.1003958.t003

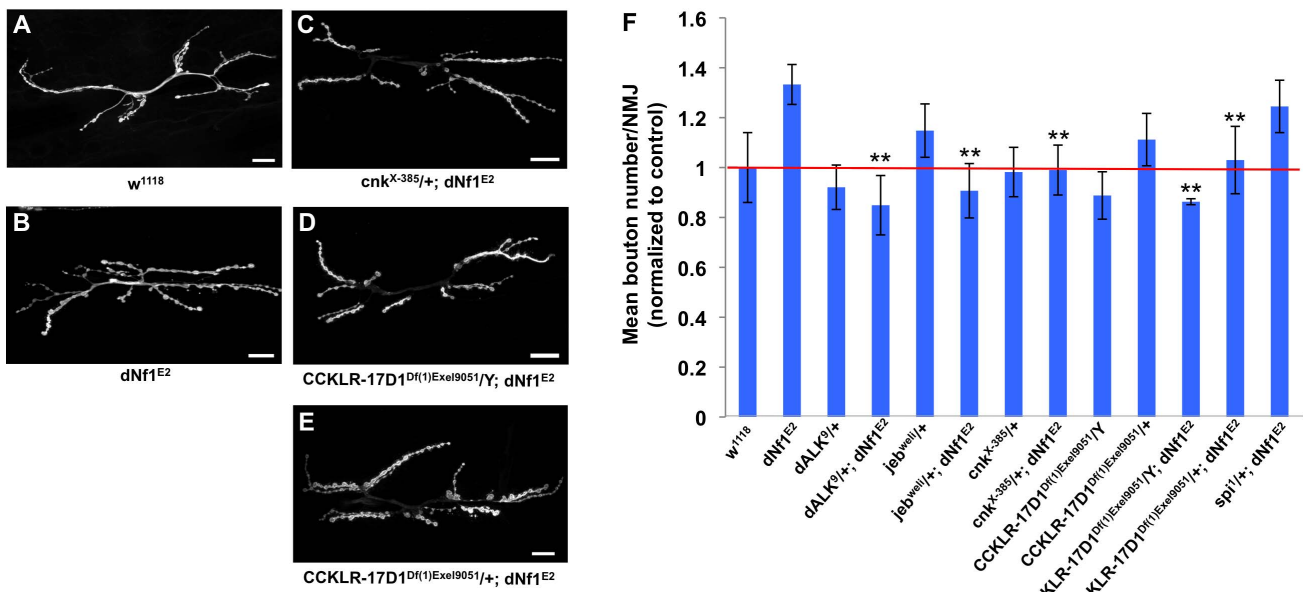


Figure 9. Several *dNf1* pupal size defect suppressors also suppress a NMJ synaptic overgrowth phenotype. (A–E) Representative micrographs of larval muscle 6/7 NMJs of the indicated genotypes. F: Mean bouton number per NMJ normalized to wild-type control. Compared to wild-type (*w¹¹¹⁸*; A), *dNf1* mutants (*dNf1^{E2}*; B) have an increased bouton number. While a *cnk* loss-of-function allele had no obvious NMJ phenotype, it dominantly suppressed the *dNf1* NMJ defect (C). Similarly, the *dNf1* NMJ phenotype was suppressed in *Df(1)Exel9051* males that lack *CCKLR-17D1* (D), while females heterozygous for *CCKLR-17D1* (E) showed a lower level of suppression. *Spitz* (*spi*) is uncovered by a modifying deficiency but does not affect *dNf1* size and was used as a negative control. In panels A–E, scale bars represent 5 μm. In panel F, error bars denote standard error of the mean. doi:10.1371/journal.pgen.1003958.g009

deficiencies were found to be lethal in a *dNf1* background (Glenn Cowley, Iswar Hariharan and A.B., unpublished), or when a pilot chemical mutagenesis screen found the reliable mapping of identified enhancer or suppressor mutations to be impracticable (Suzanne Brill, Iswar Hariharan and A.B., unpublished). Both aborted screens informed the current effort, which used precisely defined small deficiencies, isogenic crossing schemes and experimental protocols that guarded against population density differences. In total we analyzed 486 1st and 2nd chromosome deficiencies that together uncover well over 80% of chromosome 1, 2L and 2R genes (Table 1). Among the screened deficiencies, 132 (27.2%) significantly modified *dNf1* pupal size ($p < 0.01$; two-tailed Student's *t*-test). While this is a large number, 20 deficiencies were subsequently eliminated because they also affect wild-type size. Several modifying deficiencies also uncover overlapping genomic segments, further reducing the number of *dNf1* modifying loci to 76. During follow-up studies aimed at identifying responsible genes, we prioritized genes uncovered by suppressing deficiencies over those uncovered by enhancing ones, modifiers uncovered by overlapping deficiencies over those uncovered by single deletions, modifiers uncovered by small deficiencies over those uncovered by larger ones and stronger modifiers over weaker ones. We also limited ourselves to genes that function in the nervous system, based on the consideration that *dNf1* re-expression in larval neurons is sufficient to suppress the growth defect [5].

We previously reported that *dNf1* growth and learning defects are phenocopied by increasing neuronal *Jeb/dAlk/ERK* signaling, and suppressed by genetic or pharmacological attenuation of this pathway [15]. Validating our screen, deficiencies that uncover *jeb* and *dAlk* were identified as dominant *dNf1* size defect suppressors. Others recently reported that *Jeb/dAlk* signaling allows brain growth to be spared at the expense of other tissues in nutrient restricted Drosophila and identified a glial cell niche around neuroblasts as the source of *Jeb* under these conditions [41].

However, *Jeb* involved in systemic growth appears of mainly neuronal origin, as RNAi-mediated *jeb* knockdown in neurons increased *dNf1* pupal size, whereas only one of four tested glial drivers produced partial rescue (Figure 5A).

The identification of cAMP/PKA pathway modifiers *dnc*, *PKA-CI* and tentatively *PKA-R2* further validates our screen. Arguing that increased PKA activity doesn't suppress *dNf1* defects by attenuating Ras/Raf/MEK/ERK signaling, *hsp70-PKA** transgene expression, using a daily heat shock regimen that suppresses the *dNf1* size defect [4], does not reduce the elevated *dNf1* larval brain phospho-ERK level, and neither does *Ras2-Gal4* driven neuronal *UAS-PKA** expression (Figure 8D). Providing further mechanistic clues, our results demonstrate that *dNf1* and cAMP/PKA both affect systemic growth non-cell-autonomously, but not necessarily in the same cells. Thus, we previously showed that only relatively broadly expressed neuronal Gal4 drivers restored mutant growth when driving *UAS-dNf1*, whereas multiple drivers expressed in specific subsets of neurons, including several expressed in the ring gland, lacked the ability to restore *dNf1* growth [5]. By contrast, using *UAS-dnc^{RNAi}* or a series of newly generated attenuated UAS-PKA transgenes that avoid the toxicity associated with high level PKA expression [73], we now show that manipulating cAMP/PKA signaling with broadly expressed neuronal Gal drivers does not affect the *dNf1* size phenotype, whereas the same transgenes induced with three ring gland drivers did suppress. Intriguingly, the most potent rescue was observed when *UAS-dnc^{RNAi}* or attenuated *UAS-PKA** transgenes were driven in AKH-producing cells at the base of the ring gland, whereas weaker rescue was also observed with two ring gland drivers that show overlapping expression in the juvenile hormone producing corpora allata. This suggests that the *dNf1* growth deficiency involves a defect in processes controlled by one or both of these neuroendocrine hormones.

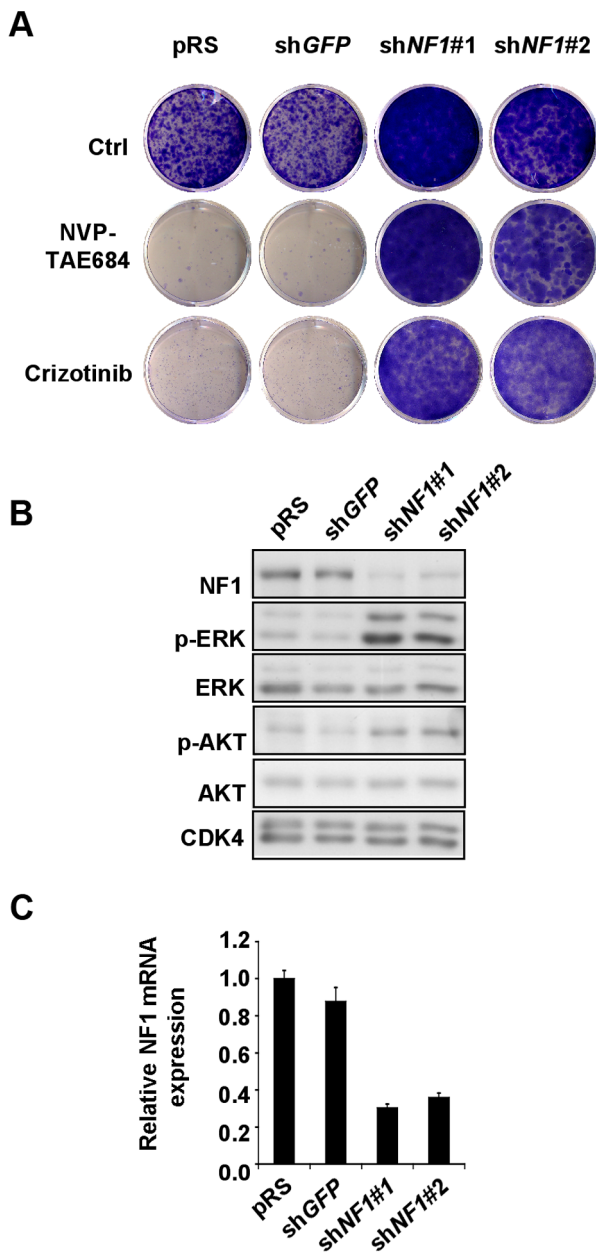


Figure 10. *NF1* suppression leads to ERK activation and confers resistance to ALK inhibitors in human neuroblastoma cells. (A) *NF1* knockdown confers resistance to ALK inhibitors in human neuroblastoma cells. SH-SY5Y cells expressing pRS and shGFP control vectors, or sh*NF1* vectors were grown in the absence or presence 50 nM NVP-TAE684 or 250 nM crizotinib. The cells were fixed, stained and photographed after 14 (untreated and crizotinib treated), or 21 (NVP-TAE684 treated) days. (B) Down-regulation of *NF1* results in elevated level of phosphorylated p-ERK and p-AKT. Western blot analysis of total lysates of SH-SY5Y cells expressing pRS, shGFP or sh*NF1* vectors. (C) The level of *NF1* knockdown by each of the RNAi vectors was measured by examining the *NF1* mRNA levels by qRT-PCR. Error bars denote standard deviation.

doi:10.1371/journal.pgen.1003958.g010

As might be expected of a screen that used systemic growth as a read-out, our work identified a diverse set of potential modifiers. Notably, however, among a non-exhaustive set of 18 1st or 2nd chromosome genes implicated in various aspects of Drosophila body, organ, and/or cell size control (*dAlk*, *B4*, *chico*, *hpo*, *Hr4*, *Ilp6*,

jeb, *Mer*, *mir-8*, *Pi3K21B*, *Pten*, *Ptth*, *SNF1A*, *sNPF*, *step*, *Tor*, *ush* and *yki*; see Table S3 for details), only *dAlk* and *jeb* scored as dominant *dNf1* pupal size modifiers, whereas the remaining 16 genes were uncovered by non-modifying deficiencies, or in the case of *Ptth*, by two deficiencies that altered developmental timing (Table S2). Further explaining this lack of overlap, the previously implicated PI3 kinase regulator *B4* act in a recessive manner and several of the above listed genes function outside of the CNS. Our screen excluded such genes, because *dNf1* controls growth non-cell-autonomously by regulating neuronal Ras [5]. As previously noted, a special case is provided by insulin pathway components *chico* and *Pten*, which affect growth antagonistically. Both genes map within 5 kb of each other on the 2nd chromosome and are uncovered by the same non-modifying deficiency.

Two newly identified *dNf1* growth defect suppressors, *Dap160* and *CCKLR-17D1*, affect synaptic architecture or functioning [36,56,57]. Because *dNf1* was recently reported to function downstream of focal adhesion kinase to restrain NMJ synaptic growth and neurotransmission [16], and because the cholecystokinin receptor related *CCKLR-17D1* drosulfakinin receptor stimulates NMJ growth [36], we analyzed whether this and three Ras signaling related *dNf1* size defect suppressors also affected NMJ architecture. Our results confirm that *dNf1* mutants exhibit synaptic overgrowth, and show that loss of *CCKLR-17D1* suppresses this defect. Importantly, loss of *jeb*, *dAlk*, or *cnk* similarly suppresses both size and synaptic overgrowth defects, suggesting that both phenotypes may be related.

The results presented here further support our previous conclusion that excess neuronal Jeb/dAlk/Ras/MEK/ERK signaling is the root cause of the cAMP/PKA sensitive *dNf1* systemic growth defect. What happens downstream of this primary defect remains less clear, although our demonstration that increasing cAMP/PKA signaling in AKH-producing cells and other parts of the neuroendocrine ring gland suppresses the size defect provides an important new clue, not only about pathways involved in the *dNf1* growth defect, but also about the likely non-cell-autonomous cause of similar growth defects of *PKA-C1* or *dCrb2* mutants [85,86]. Other questions that remain to be fully answered concern the role of the NMJ architectural defect in the *dNf1* growth deficiency and the role of Jeb/dAlk signaling in the NMJ defect. We note in this respect that that *C. elegans* ALK ortholog, *T10H9.2*, has been implicated in synapse formation [87], and that recent work suggests a role for trans-synaptic Jeb/dAlk signaling in the control of neurotransmission and synaptic morphology [88]. However, while the *dNf1* growth defect is due to excess dAlk signaling in neurons, NMJ synapse formation has been suggested to involve the release of presynaptic Jeb activating postsynaptic dAlk [88]. Further work will have to establish whether the suppression of the *dNf1* NMJ overgrowth phenotype by *jeb*, *dAlk* and *cnk* involves cell autonomous roles for these genes at synapses, or non-cell-autonomous functions elsewhere in the CNS. Further work is also required to reveal the functional significance and the sites of action of other novel modifiers identified in our screen.

From a clinical perspective, perhaps the most relevant questions raised by our work are whether *NF1* regulated ALK/RAS/ERK signaling is evolutionarily conserved and whether excessive ALK/RAS/ERK signaling contributes to human *NF1* symptoms. Much indirect evidence hints at a positive answer to both questions. First, the expression of ALK and *NF1* largely overlaps in the murine nervous system [77,78], same as it does in Drosophila [15]. Second, ALK functions as an oncogene and *NF1* as a tumor suppressor in neuroblastoma [89–94]. Third, midkine, a ligand that activates mammalian ALK [95], is produced by *NF1*^{−/−}

Schwann cells, present at elevated levels in NF1 patient skin and serum, and acts as a mitogen for NF1 tumor cell lines [96–98]. We add to this evidence by showing that shRNA-mediated *NF1* knockdown renders two oncogenic ALK-driven human neuroblastoma cell lines resistant to pharmacological ALK inhibition, and by confirming that *ALK* mRNA is expressed in neurofibromatosis-derived *NF1*^{−/−} human Schwann cells. These findings make a strong case that ALK should be explored as a therapeutic target in NF1, and that loss of *NF1* expression should be considered as a potential mechanism in cases of acquired resistance to ALK inhibition [99].

Materials and Methods

Fly Stocks and Experiments

The *dNf1^{E1}* and *dNf1^{E2}* alleles have been described [5]. Exelixis, DrosDel and BSC deficiencies were obtained from the Bloomington Stock Center. Transgenic RNAi lines were obtained from the Vienna *Drosophila* Research Center (VDRC) and the TRIP Collection at Harvard Medical School. *Eaat1^{SM1}* and *Eaat1^{SM2}* were provided by D. van Meyel, *dALK⁸* and *jeb^{weli}* by R. Palmer, *cnk^{XE-385}* and *cnk^{E-2083}* by M. Therrien, and *car^{A146}* by H. Kramer, *ppl⁰⁶⁹¹³* by M. Pankratz, *hs-Ilp2* transgenic line by E. Rulifson and *UAS-Rab9 DN* by R. Hiesinger. Flies were maintained on agar-oatmeal-molasses medium at 25°C, unless otherwise indicated.

To assess feeding, larvae at various stages of development were placed on blue food dye-stained yeast paste, removed after 20 min, washed and photographed. To analyze wandering behavior, 100 larvae (age 40–44 hr after egg deposition (AED)) were placed on an agar plate with a central blob of yeast paste, and their position after 24 hr was documented. To assess the expression of starvation-sensitive genes, larvae at 72 h AED were placed in vials with water for 16 hr, after which RNA was prepared and subjected to blot analysis. To determine developmental timing, L1 larvae were collected 24 hr AED using a 2 hr egg collection and reared at 140 animals per vial. The number of larvae that pupariated was scored at hourly intervals. To determine the larval weight, L1 larvae were collected 24 hr AED using a 2 hr egg collection. Larvae were reared at 140 larvae per vial and groups of 10 larvae were weighed at 8 hr intervals. Longevity was assessed by maintaining adult flies under standard conditions and counting the number of dead flies at regular intervals. In each of these assays, genotypes were tested in duplicate. To induce *hs-Ilp2* transgene expression, culture vials were placed in a circulating water bath at 37°C for 10 min once or twice a day with an 8 hr interval.

Insulin-Like Protein mRNA Quantification

The 7500 Fast Real-Time PCR System from Applied Biosystems was used to determine *Ilp* mRNA levels in RNA prepared from dissected larval brains or from whole wandering stage 3rd instar larvae. Results were normalized to *RpL32*. The following primers were used: *Ilp2*-Forward, GGCCAGCTCCACAGT-GAACT, *Ilp2*-Reverse, TCGCTGTCGGCACCGGGCAT, *Ilp3*-Forward, CCAGGCCACCATGAAGTTGT, *Ilp3*-Reverse, TT-GAAGTTCACGGGGTCCA, *Ilp5*-Forward, TCCGCCAG-GCCGCAAATC, *Ilp5*-Reverse, TAATCGAACAGGGCCAA-GGT, *Ilp6*-Forward, CGATGTATTCCAACAGTTTCG, *Ilp6*-Reverse, AAATCGGTTACGTTCTGCAAGTC, *Ilp7*-Forward, CAAAAAGAGGACGGGAATG, *Ilp7*-Reverse, GCCA-TCAGGTTCCGTGGTT. Expression of the distantly related *Ilp8* and the midgut-expressed *Ilp4* genes [21] was not analyzed.

Genetic Screening, Validation, and Statistical Analysis

The crossing schemes in Figure 2 were used to generate *dNf1^{E2}* mutants carrying 1st and 2nd chromosome deficiencies. To avoid crowding, cultures were maintained at 100–200 pupae per culture vial. Initial scoring used calipers set at the length of *dNf1* female pupae, ignoring *dNf1* heterozygotes recognizable by the presence of the *TM6B* balancer. Next, the length of individual pupae carrying candidate modifying deficiencies was measured by determining their head-to-tail length using a microscope fitted with NIS-Elements AR 3.0 imaging software. Measured pupae were then placed in 96-well plates (Falcon) to determine their gender and, if necessary, the genotype of eclosed flies. At least 40 pupae were measured for each genotype, and only measurements of female pupae were used to calculate mean values and standard deviations. Statistical significance was assessed with a two-tailed Student's *t*-test. Throughout this report, single or double asterisks denote *p*-values <0.05 or <0.01 respectively.

To identify responsible modifiers we used specific alleles or *UAS-RNAi* knockdown. Alleles and *UAS-RNAi* lines on the 1st and 2nd chromosomes were crossed into the *dNf1^{E2}* background. *UAS-RNAi* lines on the 3rd chromosome were recombined with *dNf1^{E2}*. *UAS-RNAi* lines in the *dNf1^{E2}* background were crossed to Gal4 drivers in the same background. The few deficiencies that gave rise to synthetic lethal interactions were backcrossed with *dNf1^{E1}* flies to produce Df/+; *dNf1^{E2}*/*dNf1^{E1}* progeny.

To test whether genetic suppression reflected the inadvertent introduction of a wild-type *dNf1* allele, we used fly DNA prepared using DNazol (Molecular Research Inc.) in a PCR assay with AGTCACATTAATTGATCCTG and GAGATCGTTGATA-AAGAAGT primers. The second primer introduces a penultimate single nucleotide change, which together with the E2 mutation results in the introduction of an RsaI restriction site. RsaI digestion of the PCR product gives rise to 370 and 61 bp fragments for the wild-type allele, and 348, 61 and 22 bp fragments for the *dNf1^{E2}* allele. Digests were run on 8% acrylamide gels using both wild-type (*w¹¹¹⁸*) and *dNf1^{E2}* controls.

Construction of *Akh-Gal4* and Attenuated *UAS-PKA** Transgenes

The *Akh* promoter region was amplified with *Akh*-FORWARD (AGATCTAATCTCCTGAATGCCGAGCG) and *Akh*-REVERSE (AGATCTATGCTGGTCCACTTCGATTTC) primers. The resulting PCR fragment was subcloned into the BamHI site of a GAL4 coding region containing pCaSpeR derivative. The final construct was sequenced to ensure correct orientation of the *Akh* promoter before being used to generate transgenic flies by standard protocols.

To reduce the toxicity associated with high-level PKA expression, we generated modified pUAS-T vectors containing 1, 2, 3 or 4, rather than 5 Gal4-binding sites. The primers used to generate these vectors were: 1×UAS-FOR: AACTGCAGAGCG-GAGTACTGTCCTCCGAGCGGAGACTCTAG; 2×UAS-FOR: AACTGCAGCGGAGTACTGTCCTCCGAGCGGAG-TACTGTCCTCCG; 3×UAS-FOR: AACTGCAGCGGAG-TACTGTCCTCCGAGCGGAGACTGTCCTCCGAGCGGAGACTGTCCTCCG, and UAS-REV: CTAGAGGTAC-CCTCGAGCGGGCCGCAAGAT. An initial PCR was performed using the 1×UAS-FOR and UAS-REV primers with the standard pUAS-T vector as a template. The resulting amplified fragment was TA subcloned into pCR2.1 to make pCR2.1-1×UAS. The 2×UAS-FOR and UAS-REV primers were then used with pCR2.1-UAS(1×) as a template to generate a UAS(2×) clone, which was subcloned to produce pCR2.1-UAS(2×). Similarly, 3×UAS-FOR and UAS-REV primers in a PCR

reaction with pCR2.1-UAS(2 \times) as template generated pCR2.1-UAS(3 \times) and pCR2.1-UAS(4 \times). The pCR2.1-UAS clones were sequenced, their inserts excised with PstI and subcloned into PstI-digested p-UAST. Correct insert orientation was verified by sequence analysis, after which the mutationally activated murine PKA* coding region [100] was subcloned into the modified vectors using XbaI and NotI.

Immunofluorescence and Analysis of NMJ Morphology

Wandering third instar larvae were dissected in Ca²⁺-free saline and fixed in 4% paraformaldehyde for 25 min at room temperature. Following fixation, larval peels were washed three times in phosphate-buffered saline (PBS) and then blocked for one hour in PBT (PBS+0.1% Triton-X 100)+5% normal goat serum. Larvae were incubated in primary antibody solution for three hours at room temperature. Anti-HRP 568 (1:1000, Invitrogen) was used to visualize neurons and Alexa Fluor 488 phalloidin (1:500, Invitrogen) was used to visualize F-actin in the musculature. Images were collected using a Yokogawa CSU-X1 spinning-disk confocal microscope with the Spectral Applied Research (Richmond Hill, ON, Canada) Borealis modification on a Nikon (Melville, NY) Ti-E inverted microscope using a 60 \times Plan Apo (1.4 NA) objective. The microscope was equipped with a Prior (Rockland, MA) Proscan II motorized stage. Larval samples were excited with 488-nm (for phalloidin) and 561-nm (for HRP) 100-mW solid-state lasers from a Spectral Applied Research LMM-5 laser merge module and was selected and controlled with an acousto-optical tunable filter. Emission was collected with a Semrock (Rochester, NY) quad pass (405/491/561/642 nm) dichroic mirror and 525/50 nm (for phalloidin) and 620/60 nm (for HRP) Chroma (Bellows Falls, VT) emission filters. Images were acquired using a Hamamatsu ORCA-ER-cooled CCD camera. Hardware was controlled with MetaMorph (version 7.7.9) software (Molecular Devices, Sunnyvale, CA.). Five individual animals were imaged for subsequent morphological analysis. Motor nerve terminals of muscles 6 and 7 were imaged in abdominal segments A2 and A3 and Z-stacks (0.25 μ M between images) and were captured from the top to bottom of each NMJ. Morphological analysis of the NMJ was performed using NIH Image J and was assessed by quantifying the number of synaptic boutons per square micron. The number of synaptic boutons was counted as previously described [16,101] and muscle area covered by the NMJ was quantified by tracing a polygon connecting each terminal branch point [102].

Human NF1 Experiments

The retroviral RNAi vectors targeting human *NF1* and expression constructs of active alleles of RAS effectors were as described previously [94]. Crizotinib (S1068) and NVP-TAE648 (S1108) were purchased from Selleck Chemicals. Antibody against NF1 was from Bethyl Laboratories (A300-140A); antibodies against pAKT(S473) and ATK1/2 were from Cell Signalling; antibodies against p-ERK (E-4), ERK1 (C-16), ERK2 (C-14) and CDK4 (C-22) were from Santa Cruz Biotechnology; A mixture of ERK1 and ERK2 antibodies was used for detection of total ERK from human cell lines. Antibody against mouse PKA α -cat (A-2) SC-28315 was from Santa Cruz Biotechnology, β -Tubulin E7 from Developmental Studies Hybridoma Bank.

SH-SY5Y, Kelly and Phoenix cells were cultured in DMEM with 8% heat-inactivated fetal bovine serum, penicillin and streptomycin at 5% CO₂. Subclones of each cell line expressing the murine ecotropic receptor were generated and used for all experiments shown. Phoenix cells were used to produce retroviral

supernatants as described at http://www.stanford.edu/group/nolan/retroviral_systems/phx.html.

To measure cell proliferation, single cell suspensions were seeded into 6-well plates (1–2 \times 10⁴ cells/well) and cultured both in the absence and presence of ALK inhibitors. At the indicated endpoints, cells were fixed, stained with crystal violet and photographed. All knockdown and overexpression experiments were done by retroviral infection as described previously [103].

The 7500 Fast Real-Time PCR System from Applied Biosystems was used to determine mRNA levels. *NF1* mRNA expression levels were normalized to expression of *GAPDH*. The following primers sequences were used in the SYBR Green master mix (Roche): *GAPDH*-Forward, AAGGTGAAGGTCGGAGTC; *GAPDH*-Reverse, AATGAAGGGGTCTTGATGG; *NF1*-Forward, TGTCACTGCATAACCTCTTC; *NF1*-Reverse, AGT-GCCATCACTCTTCTGAAG. *ALK* mRNA levels in neurofibroma-derived *NF1*^{−/−} Schwann cells and *NF1*^{+/−} fibroblasts were analyzed using the following two primer sets: *ALK*-N-Forward, GGAGTCAGCTGAGGTGTTG; *ALK*-N-Reverse, TGGAGTCAGCTGAGGTGTTG; *ALK*-C-Forward, GCAAC-ATCACGCTGAAGACA; *ALK*-C-Reverse, GCCTGTTGAGA-GACCAGGAG.

Supporting Information

Figure S1 Loss of *dNf1* does not alter developmental timing but reduces larval growth rate. (A) Wild-type, *dNf1*^{E1}, and *dNf1*^{E1/E2} mutants show no altered developmental timing, as judged by their rate of pupariation (also shown in Figure 1D). By contrast, larvae with *phm-Gal4* driving *UAS-Ras1*^{V12} undergo accelerated development resulting in miniature pupae [104], whereas *phm-Gal4* driving a dominant negative *UAS-P13K*^{D954A} transgene delayed development and produced giant pupae [71]. (B) Mouth hook length measurements (in μ m) show that *dNf1* larvae grow at a reduced rate. The marker represents the mean length; the upper box represents the median to Q3 value, the lower box median to Q1 value and the error bars identify the outliers.

(PDF)

Figure S2 PCR/RFLP assay for *dNf1*^{E2} mutation. (A) To make sure that stocks with putative suppressing deficiencies preserved the *dNf1*^{E2} C->T nonsense transition, we used a PCR/Restriction Fragment Length Polymorphism assay. The E2 mutation does not create or destroy a restriction site. Rather, we used a reverse primer with a penultimate A->C transversion to amplify a 431 genomic fragment as indicated. The mutant primer creates a GTAC RsaI restriction site when E2 genomic DNA is used as a template. (B) RsaI digestion of PCR products gives rise to 370 and 61 bp fragments for the wild-type allele, and 348, 61 and 22 bp fragments for *dNf1*^{E2}. An example of the assay is shown with both wild-type (*w¹¹¹⁸*) and *dNf1*^{E2} controls (lanes 2, 3 and 4) and various deficiencies (Df) either in wild-type (*Df/CyO*; +; lanes 5 and 15), *dNf1* homozygous (*Df/CyO*; *dNf1*^{E2}; lanes 6–13) or heterozygous (*Df/CyO*; *dNf1*^{E2}/+; lanes 14 and 16) backgrounds.

(PDF)

Figure S3 Systematic identification for *dNf1* modifiers. For deficiencies that did not uncover obvious candidate modifier genes, a systematic RNAi approach was used. UAS-RNAi lines targeting genes uncovered by a modifying deficiency were driven by *Ras2-Gal4* in the *dNf1*^{E2} background and the effect on pupal size determined. (A) Identification of *carnation* as a *dNf1* modifier uncovered by suppressing *Df(1)BSC275*. (B) Identification of *NAATT1* as the responsible gene uncovered by suppressing deficiencies *Df(1)BSC533* and *Df(1)Exel6290*. RNAi-induced

lethality is denoted by †. Error bars show standard deviations and * indicates a *p*-value of <0.05. As part of the systematic identification of modifiers 385 RNAi lines were tested.

(PDF)

Figure S4 The *Ret* tyrosine kinase is not involved in *dNf1* growth control. (A) Reagents generated to analyze the involvement of *Ret* include *Ret-Gal4* transgenic lines made by inserting a 957-bp genomic segment representing the *Ret* promoter region into the pChs-*Gal4* vector. Other reagents include *UAS-Ret* transgenes harboring kinase-dead (K805A) and constitutively active (C695R) mutations made by site-directed mutagenesis. (B) *Ret-Gal4* driven *UAS-GFP* expression recapitulates the endogenous larval brain *Ret* expression pattern [60]. (C) *GMR-Gal4* driven *UAS-Ret* with a constitutively active C695R mutation produces a rough eye phenotype as previously reported [60]. (D) *Ret-Gal4* driven *UAS-dNf1* re-expression, RNAi-mediated *Ret* inhibition or expression of a *UAS-Ret* kinase dead transgene, all failed to modify *dNf1* pupal size. Moreover, *Ret-Gal4* driven expression of *UAS-Ret* with constitutively active C695R mutation failed to phenocopy the *dNf1* size defect. By contrast, a small pupal size phenocopy was observed when *Ret* C695R was driven ectopically with *Ras2*- and *elav-Gal4*, likely reflecting *Ret*-mediated activation of Ras/ERK signaling.

(PDF)

Figure S5 Expression pattern of ring gland drivers. Ring gland drivers *P0206-Gal4*, *Feb36-Gal4*, *Aug21-Gal4* and *Akh-Gal4* were crossed to *UAS-GFP*. The CNS and ring glands were dissected from third instar larvae, stained with DAPI and imaged using confocal microscopy. The prothoracic gland (PG), corpora allatula (CA) and corpora cardiaca (CC) are indicated. Specimens are orientated such that the base of the brain hemispheres is at the top, indicated by a dotted line. Scale bar = 50 μm.

(PDF)

Figure S6 ALK mRNA expression in neurofibroma-derived Schwann cells. Reverse transcription/PCR was used to analyze ALK expression in neurofibroma-derived *NFI*^{−/−} Schwann cells and *NFI*^{+/−} fibroblasts. Two primer sets, (A) ALK-N and (B) ALK-C, designed to amplify N-terminal and C-terminal ALK mRNA segments, detected ALK expression in *NFI*^{−/−} Schwann cells, but not in *NFI*^{+/−} fibroblasts. *GAPDH* primers were used as a control. To guard against positive signals due to contaminating genomic DNA, each PCR reaction was set up either with (+RT) or without (−RT) reverse transcriptase.

(PDF)

Figure S7 *NF1* suppression confers resistance to ALK inhibitors in human neuroblastoma cells. (A) Kelly cells expressing pRS and sh*GFP* controls or sh*NF1* vectors were grown in the absence or presence 200 nM NVP-TAE684 or 500 nM crizotinib. Cells were fixed, stained and photographed after 14 (untreated) or 17 (NVP-TAE684 or crizotinib-treated) days. (B) Level of *NF1* knockdown assayed by qRT-PCR. Error bars denote standard deviation.

(PDF)

Figure S8 Activation of RAS-RAF-MEK cascade confers resistance to ALK inhibitors in neuroblastoma cells. (A) Constitutively active *KRAS*^{V12}, *BRAF*^{V600E} or *MEK1*^{S218D,S222D} mutants confer resistance to ALK inhibitors. SH-SY5Y neuroblastoma cells expressing pBabe vector control or the indicated active RAS effector mutants were grown in the absence or presence 50 nM NVP-TAE684 or 350 nM crizotinib. The cells were fixed, stained and photographed after 12 (untreated) or 19 (NVP-TAE684 and crizotinib-treated) days. (B) Level of phosphorylated ERK and AKT in the SH-SY5Y cells described above.

(PDF)

Table S1 Excluded deficiencies. Listed deficiencies were excluded for the reasons indicated. Deficiencies that failed to produce screening stocks are labeled ‘Impossible’. Unhealthy (sick) deficiencies or those that uncovered *Minute* mutations were also excluded.

(PDF)

Table S2 *dNf1* modifier deficiency screen results. All deficiencies analyzed are listed according to their relative chromosomal position. The cytological location, molecular coordinates and the dominant effect on *dNf1* pupal size (NO – no interaction, SUP - suppressor, ENH - enhancer) of each deficiency is given. Female pupal length measurements for deficiencies in the *dNf1* mutant background are provided, together with standard deviations and *p*-values. Modifying deficiencies that were subsequently found to have an effect on wild-type pupal size are indicated (Yes – indicates that a deficiency has a non-specific effect; No – no observed effect on wild-type size; No* - has an effect on wild-type size, but in the opposite direction from the effect on *dNf1* mutants). Where determined, the responsible gene identified under each modifying deficiency is shown. The final column contains notes such as deficiencies that result in altered developmental timing.

(PDF)

Table S3 Growth related genes uncovered by screened deficiencies. 18 cell, tissue, or systemic growth implicated genes uncovered by analyzed 1st and 2nd chromosome deficiencies. Among the deficiencies listed, only those that uncovered *dAlk* or *jeb* modified *dNf1* pupal size.

(PDF)

Table S4 Larval tissue expression patterns of Gal4 drivers. List of Gal4 driver lines used in this study and their expression patterns in third instar larvae as determined by crossing Gal4 drivers to *UAS-GFP*, or from published data. Abbreviations: Ring gland (RG), central nervous system (CNS), mushroom body (MB), prothoracic gland (PG), corpora allata (CA), corpora cardiaca (CC), neurosecretory neurons (NSNs), pars intercerebralis neurons (PI), corpora cardiaca innervating neurosecretory neuron of the medial subesophageal ganglion 2 (CC-MS 2), proventriculus (PV), fat body (FB), salivary glands (SG), imaginal discs (IDs), first instar (L1).

(PDF)

Table S5 Identification of tissues that require *dNf1* or cAMP/PKA signaling for growth regulation. Various Gal4 drivers in the *dNf1* background were crossed to *dNf1* mutants bearing attenuated *UAS-PKA** transgenes or *dnc* RNAi lines. Rescue was assessed by measuring pupae, followed by genotyping adult flies upon eclosion. All crosses produced viable adults unless otherwise stated. † denotes lethality; NR non-rescue; NR* denotes non-rescue with adult eclosers with unfurled wings; n/a not applicable; n/d not determined.

(PDF)

Acknowledgments

We thank the Bloomington Drosophila Stock and Vienna Drosophila Resource Centers for deficiency and transgenic RNAi fly stocks. We are also grateful to R. Hiesinger, H. Kramer, D. van Meyel, R. Palmer and M. Therrien for additional fly stocks, to Spyros Artavanis-Tsakonas and Doug Dimlich for Exelixis deficiency stocks, and to Eline Beert and Eric Legius for *NF1* tumor cell RNAs. We are grateful to the Nikon Imaging Center at Harvard Medical School for technical support for microscopy performed in this study. Transgenic flies were generated by Genetic Services Inc., Cambridge MA. We thank Iswar Hariharan, Susanne Brill and Glenn Cowley for their efforts during the early stages of this project, and our colleagues at the MGH Center for Cancer Research for valuable discussions.

Author Contributions

Conceived and designed the experiments: JAW JYG SH JBL DVV RB AB. Performed the experiments: JAW JYG JBL SH RCM HX KK AR.

References

1. Zenker M (2011) Clinical manifestations of mutations in RAS and related intracellular signal transduction factors. *Current opinion in pediatrics* 23: 443–451.
2. Evans DG, Howard E, Giblin C, Clancy T, Spencer H, et al. (2010) Birth incidence and prevalence of tumor-prone syndromes: estimates from a UK family genetic register service. *American journal of medical genetics Part A* 152A: 327–332.
3. Allanson JE (2007) Noonan syndrome. *American journal of medical genetics Part C, Seminars in medical genetics* 145C: 274–279.
4. The I, Hannigan GE, Cowley GS, Reginald S, Zhong Y, et al. (1997) Rescue of a Drosophila NF1 mutant phenotype by protein kinase A. *Science* 276: 791–794.
5. Walker JA, Tchoudakova AV, McKenney PT, Brill S, Wu D, et al. (2006) Reduced growth of Drosophila neurofibromatosis 1 mutants reflects a non-cell-autonomous requirement for GTPase-Activating Protein activity in larval neurons. *Genes & development* 20: 3311–3323.
6. Guo HF, The I, Hannan F, Bernards A, Zhong Y (1997) Requirement of Drosophila NF1 for activation of adenylyl cyclase by PACAP38-like neuropeptides. *Science* 276: 795–798.
7. Hyman SL, Shores A, North KN (2005) The nature and frequency of cognitive deficits in children with neurofibromatosis type 1. *Neurology* 65: 1037–1044.
8. Silva AJ, Frankland PW, Marowitz Z, Friedman E, Laszlo GS, et al. (1997) A mouse model for the learning and memory deficits associated with neurofibromatosis type I. *Nature genetics* 15: 281–284.
9. Guo HF, Tong J, Hannan F, Luo L, Zhong Y (2000) A neurofibromatosis-1-regulated pathway is required for learning in Drosophila. *Nature* 403: 895–898.
10. Hannan F, Ho I, Tong JJ, Zhu Y, Nurnberg P, et al. (2006) Effect of neurofibromatosis type I mutations on a novel pathway for adenylyl cyclase activation requiring neurofibromin and Ras. *Human molecular genetics* 15: 1087–1098.
11. Tong J, Hannan F, Zhu Y, Bernards A, Zhong Y (2002) Neurofibromin regulates G protein-stimulated adenylyl cyclase activity. *Nature neuroscience* 5: 95–96.
12. Brown JA, Gianino SM, Gutmann DH (2010) Defective cAMP generation underlies the sensitivity of CNS neurons to neurofibromatosis-1 heterozygosity. *The Journal of neuroscience: the official journal of the Society for Neuroscience* 30: 5579–5589.
13. Dasgupta B, Dugan LL, Gutmann DH (2003) The neurofibromatosis 1 gene product neurofibromin regulates pituitary adenylate cyclase-activating polypeptide-mediated signaling in astrocytes. *The Journal of neuroscience: the official journal of the Society for Neuroscience* 23: 8949–8954.
14. Ho IS, Hannan F, Guo HF, Hakker I, Zhong Y (2007) Distinct functional domains of neurofibromatosis type 1 regulate immediate versus long-term memory formation. *The Journal of neuroscience: the official journal of the Society for Neuroscience* 27: 6852–6857.
15. Gouzi JY, Moressi A, Walker JA, Apostolopoulou AA, Palmer RH, et al. (2011) The receptor tyrosine kinase Alk controls neurofibromin functions in Drosophila growth and learning. *PLoS genetics* 7: e1002281.
16. Tsai PI, Wang M, Kao HH, Cheng YJ, Walker JA, et al. (2012) Neurofibromin Mediates FAK Signaling in Confining Synapse Growth at Drosophila Neuromuscular Junctions. *The Journal of neuroscience: the official journal of the Society for Neuroscience* 32: 16971–16981.
17. Ashburner M, Thompson JN (1978) The laboratory culture of Drosophila. In: Ashburner M, Wright TRF, editors. *The Genetics and Biology of Drosophila*. London: Academic Press. pp. 1–109.
18. Zinke I, Kirchner C, Chao LC, Tetzlaff MT, Pankratz MJ (1999) Suppression of food intake and growth by amino acids in Drosophila: the role of pumpless, a fat body expressed gene with homology to vertebrate glycine cleavage system. *Development* 126: 5275–5284.
19. Mirth CK, Shingleton AW (2012) Integrating body and organ size in Drosophila: recent advances and outstanding problems. *Frontiers in endocrinology* 3: 49.
20. Andersen DS, Colombani J, Leopold P (2013) Coordination of organ growth: principles and outstanding questions from the world of insects. *Trends in cell biology* 23(7):336–44.
21. Brogiolo W, Stocker H, Ikeya T, Rintelen F, Fernandez R, et al. (2001) An evolutionarily conserved function of the Drosophila insulin receptor and insulin-like peptides in growth control. *Current biology*: CB 11: 213–221.
22. Ikeya T, Galic M, Belawat P, Nairz K, Hafen E (2002) Nutrient-dependent expression of insulin-like peptides from neuroendocrine cells in the CNS contributes to growth regulation in Drosophila. *Current biology*: CB 12: 1293–1300.
23. Rulifson EJ, Kim SK, Nusse R (2002) Ablation of insulin-producing neurons in flies: growth and diabetic phenotypes. *Science* 296: 1118–1120.
24. Hwangbo DS, Gershman B, Tu MP, Palmer M, Tatar M (2004) Drosophila dFOXO controls lifespan and regulates insulin signalling in brain and fat body. *Nature* 429: 562–566.
25. Clancy DJ, Gems D, Harshman LG, Oldham S, Stocker H, et al. (2001) Extension of life-span by loss of CHICO, a Drosophila insulin receptor substrate protein. *Science* 292: 104–106.
26. Tatar M, Kopelman A, Epstein D, Tu MP, Yin CM, et al. (2001) A mutant Drosophila insulin receptor homolog that extends life-span and impairs neuroendocrine function. *Science* 292: 107–110.
27. Tong JJ, Schriner SE, McCleary D, Day BJ, Wallace DC (2007) Life extension through neurofibromin mitochondrial regulation and antioxidant therapy for neurofibromatosis-1 in Drosophila melanogaster. *Nature genetics* 39: 476–485.
28. Artavanis-Tsakonas S (2004) Accessing the Exelixis collection. *Nature genetics* 36: 207.
29. Ryder E, Ashburner M, Bautista-Llacer R, Drummond J, Webster J, et al. (2007) The DrosDel deletion collection: a Drosophila genome-wide chromosomal deficiency resource. *Genetics* 177: 615–629.
30. Schultz J (1929) The Minute Reaction in the Development of DROSOPHILA MELANOGASTER. *Genetics* 14: 366–419.
31. Marygold SJ, Roote J, Reuter G, Lambertsson A, Ashburner M, et al. (2007) The ribosomal protein genes and Minute loci of Drosophila melanogaster. *Genome biology* 8: R216.
32. Dietzl G, Chen D, Schnorrer F, Su KC, Baranova Y, et al. (2007) A genome-wide transgenic RNAi library for conditional gene inactivation in Drosophila. *Nature* 448: 151–156.
33. Gutierrez E, Wiggins D, Fielding B, Gould AP (2007) Specialized hepatocyte-like cells regulate Drosophila lipid metabolism. *Nature* 445: 275–280.
34. Tennessen JM, Thummel CS (2011) Coordinating growth and maturation – insights from Drosophila. *Current biology*: CB 21: R750–757.
35. Williams JA, Su HS, Bernards A, Field J, Sehgal A (2001) A circadian output in Drosophila mediated by neurofibromatosis-1 and Ras/MAPK. *Science* 293: 2251–2256.
36. Chen X, Ganetzky B (2012) A neuropeptide signaling pathway regulates synaptic growth in Drosophila. *The Journal of cell biology* 196: 529–543.
37. Gorokhova S, Bibert S, Geering K, Heintz N (2007) A novel family of transmembrane proteins interacting with beta subunits of the Na,K-ATPase. *Human molecular genetics* 16: 2394–2410.
38. Miller MM, Popova LB, Meleshevitch EA, Tran PV, Boudko DY (2008) The invertebrate B(0) system transporter, D. melanogaster NAT1, has unique d-amino acid affinity and mediates gut and brain functions. *Insect biochemistry and molecular biology* 38: 923–931.
39. Kamimura K, Rhodes JM, Ueda R, McNely M, Shukla D, et al. (2004) Regulation of Notch signaling by Drosophila heparan sulfate 3-O sulfotransferase. *The Journal of cell biology* 166: 1069–1079.
40. Loren CE, Scully A, Grabbe C, Edeen PT, Thomas J, et al. (2001) Identification and characterization of DAlk: a novel Drosophila melanogaster RTK which drives ERK activation in vivo. *Genes to cells: devoted to molecular & cellular mechanisms* 6: 531–544.
41. Cheng LY, Bailey AP, Leevers SJ, Ragan TJ, Driscoll PC, et al. (2011) Anaplastic lymphoma kinase spares organ growth during nutrient restriction in Drosophila. *Cell* 146: 435–447.
42. Stute C, Schimmelpfeng K, Renkawitz-Pohl R, Palmer RH, Holz A (2004) Myoblast determination in the somatic and visceral mesoderm depends on Notch signalling as well as on milliways(mili(Alk)) as receptor for Jeb signalling. *Development* 131: 743–754.
43. Lu X, Melnick MB, Hsu JC, Perrimon N (1994) Genetic and molecular analyses of mutations involved in Drosophila raf signal transduction. *The EMBO journal* 13: 2592–2599.
44. Simon MA, Bowtell DD, Dodson GS, Laverty TR, Rubin GM (1991) Ras1 and a putative guanine nucleotide exchange factor perform crucial steps in signaling by the sevenless protein tyrosine kinase. *Cell* 67: 701–716.
45. Dickson BJ, van der Straten A, Dominguez M, Hafen E (1996) Mutations Modulating Raf signaling in Drosophila eye development. *Genetics* 142: 163–171.
46. Karim FD, Chang HC, Therrien M, Wasserman DA, Laverty T, et al. (1996) A screen for genes that function downstream of Ras1 during Drosophila eye development. *Genetics* 143: 315–329.
47. Maixner A, Hecker TP, Phan QN, Wasserman DA (1998) A screen for mutations that prevent lethality caused by expression of activated sevenless and Ras1 in the Drosophila embryo. *Developmental genetics* 23: 347–361.
48. Huang AM, Rubin GM (2000) A misexpression screen identifies genes that can modulate RAS1 pathway signaling in Drosophila melanogaster. *Genetics* 156: 1219–1230.
49. Rebay I, Chen F, Hsiao F, Kolodziej PA, Kuang BH, et al. (2000) A genetic screen for novel components of the Ras/Mitogen-activated protein kinase signaling pathway that interact with the yan gene of Drosophila identifies split

- ends, a new RNA recognition motif-containing protein. *Genetics* 154: 695–712.
50. Zhu MY, Wilson R, Leptin M (2005) A screen for genes that influence fibroblast growth factor signal transduction in *Drosophila*. *Genetics* 170: 767–777.
 51. Friedman A, Perrimon N (2006) A functional RNAi screen for regulators of receptor tyrosine kinase and ERK signalling. *Nature* 444: 230–234.
 52. Friedman AA, Tucker G, Singh R, Yan D, Vinayagam A, et al. (2011) Proteomic and functional genomic landscape of receptor tyrosine kinase and ras to extracellular signal-regulated kinase signaling. *Science signaling* 4: rs10.
 53. Therrien M, Wong AM, Rubin GM (1998) CNK, a RAF-binding multidomain protein required for RAS signaling. *Cell* 95: 343–353.
 54. Douziech M, Roy F, Laberge G, Lefrancois M, Armengod AV, et al. (2003) Bimodal regulation of RAF by CNK in *Drosophila*. *The EMBO journal* 22: 5068–5078.
 55. Roos J, Kelly RB (1998) Dap160, a neural-specific Eps15 homology and multiple SH3 domain-containing protein that interacts with *Drosophila* dynamin. *The Journal of biological chemistry* 273: 19108–19119.
 56. Koh TW, Verstreken P, Bellen HJ (2004) Dap160/intersectin acts as a stabilizing scaffold required for synaptic development and vesicle endocytosis. *Neuron* 43: 193–205.
 57. Marie B, Sweeney ST, Poskanzer KE, Roos J, Kelly RB, et al. (2004) Dap160/intersectin scaffolds the periactive zone to achieve high-fidelity endocytosis and normal synaptic growth. *Neuron* 43: 207–219.
 58. Chabu C, Doe CQ (2008) Dap160/intersectin binds and activates aPKC to regulate cell polarity and cell cycle progression. *Development* 135: 2739–2746.
 59. Opochev G, Conton P, Schiavi F, Macino B, Mantero F (2005) Pheochromocytoma in von Hippel-Lindau disease and neurofibromatosis type 1. *Familial cancer* 4: 13–16.
 60. Read RD, Goodfellow PJ, Mardis ER, Novak N, Armstrong JR, et al. (2005) A *Drosophila* model of multiple endocrine neoplasia type 2. *Genetics* 171: 1057–1081.
 61. Chan CC, Scoggin S, Wang D, Cherry S, Dembo T, et al. (2011) Systematic discovery of Rab GTPases with synaptic functions in *Drosophila*. *Current biology*: CB 21: 1704–1715.
 62. Bekker-Jensen S, Rendtlew Danielsen J, Fugger K, Gromova I, Nerstedt A, et al. (2010) HERC2 coordinates ubiquitin-dependent assembly of DNA repair factors on damaged chromosomes. *Nature cell biology* 12: 80–86; sup pp 81–12.
 63. Sevrioukov EA, He JP, Moghrabi N, Sunio A, Kramer H (1999) A role for the deep orange and carnation eye color genes in lysosomal delivery in *Drosophila*. *Molecular cell* 4: 479–486.
 64. Pulpipparacharuvil S, Akbar MA, Ray S, Sevrioukov EA, Haberman AS, et al. (2005) *Drosophila* Vps16A is required for trafficking to lysosomes and biogenesis of pigment granules. *Journal of cell science* 118: 3663–3673.
 65. Wittwer F, Jaquenoud M, Brogiolo W, Zarske M, Wustemann P, et al. (2005) Susi, a negative regulator of *Drosophila* PI3-kinase. *Developmental cell* 8: 817–827.
 66. Okamoto N, Yamanaka N, Yagi Y, Nishida Y, Kataoka H, et al. (2009) A fat body-derived IGF-like peptide regulates postfeeding growth in *Drosophila*. *Developmental cell* 17: 885–891.
 67. Slaidina M, Delanoue R, Gronke S, Partridge L, Leopold P (2009) A *Drosophila* insulin-like peptide promotes growth during nonfeeding states. *Developmental cell* 17: 874–884.
 68. Bohni R, Riesgo-Escovar J, Oldham S, Brogiolo W, Stocker H, et al. (1999) Autonomous control of cell and organ size by CHICO, a *Drosophila* homolog of vertebrate IRS1-4. *Cell* 97: 865–875.
 69. Goberdhan DC, Paricio N, Goodman EC, Mlodzik M, Wilson C (1999) *Drosophila* tumor suppressor PTEN controls cell size and number by antagonizing the Chico/PI3-kinase signaling pathway. *Genes & development* 13: 3244–3258.
 70. King-Jones K, Charles JP, Lam G, Thummel CS (2005) The ecdysone-induced DHR4 orphan nuclear receptor coordinates growth and maturation in *Drosophila*. *Cell* 121: 773–784.
 71. Mirth C, Truman JW, Riddiford LM (2005) The role of the prothoracic gland in determining critical weight for metamorphosis in *Drosophila melanogaster*. *Current biology*: CB 15: 1796–1807.
 72. McBrayer Z, Ono H, Shimell M, Parvy JP, Beckstead RB, et al. (2007) Prothoracotrophic hormone regulates developmental timing and body size in *Drosophila*. *Developmental cell* 13: 857–871.
 73. Kiger JA Jr., Eklund JL, Younger SH, O'Kane CJ (1999) Transgenic inhibitors identify two roles for protein kinase A in *Drosophila* development. *Genetics* 152: 281–290.
 74. Walker JA, Gouzi JY, Huang S, Maher R, Xia H, et al. (2013) A Genetic Screen For Genes Involved In The *Drosophila* Neurofibromatosis-1 Growth Defect Implicates ALK And Other Potential Therapeutic Targets. *PLoS genetics*. In Press.
 75. Keshishian H, Broadie K, Chiba A, Bate M (1996) The *Drosophila* neuromuscular junction: a model system for studying synaptic development and function. *Annual review of neuroscience* 19: 545–575.
 76. Rohrbough J, Broadie K (2010) Anterograde Jelly belly ligand to Alk receptor signaling at developing synapses is regulated by Mind the gap. *Development* 137: 3523–3533.
 77. Daston MM, Ratner N (1992) Neurofibromin, a predominantly neuronal GTPase activating protein in the adult, is ubiquitously expressed during development. *Developmental dynamics: an official publication of the American Association of Anatomists* 195: 216–226.
 78. Iwahara T, Fujimoto J, Wen D, Cupples R, Bucay N, et al. (1997) Molecular characterization of ALK, a receptor tyrosine kinase expressed specifically in the nervous system. *Oncogene* 14: 439–449.
 79. Serra E, Rosenbaum T, Winner U, Alejo R, Ars E, et al. (2000) Schwann cells harbor the somatic NF1 mutation in neurofibromas: evidence of two different Schwann cell subpopulations. *Human molecular genetics* 9: 3055–3064.
 80. McDermott U, Iafrate AJ, Gray NS, Shioda T, Classon M, et al. (2008) Genomic alterations of anaplastic lymphoma kinase may sensitize tumors to anaplastic lymphoma kinase inhibitors. *Cancer research* 68: 3389–3395.
 81. Easton DF, Ponder MA, Huson SM, Ponder BA (1993) An analysis of variation in expression of neurofibromatosis (NF) type 1 (NF1): evidence for modifying genes. *American journal of human genetics* 53: 305–313.
 82. Soucy EA, Van Oppen D, Nejedly NL, Gao F, Gutmann DH, et al. (2012) Height Assessments in Children With Neurofibromatosis Type 1. *Journal of child neurology* 28(3):303–7.
 83. Stowe IB, Mercado EL, Stowe TR, Bell EL, Oses-Prieto JA, et al. (2012) A shared molecular mechanism underlies the human rasopathies Legius syndrome and Neurofibromatosis-1. *Genes & development* 26: 1421–1426.
 84. Grewal SS (2012) Controlling animal growth and body size - does fruit fly physiology point the way? *F1000 biology reports* 4: 12.
 85. Lane ME, Kalderon D (1993) Genetic investigation of cAMP-dependent protein kinase function in *Drosophila* development. *Genes & development* 7: 1229–1243.
 86. Belvin MP, Zhou H, Yin JC (1999) The *Drosophila* dCREB2 gene affects the circadian clock. *Neuron* 22: 777–787.
 87. Liao EH, Hung W, Abrams B, Zhen M (2004) An SCF-like ubiquitin ligase complex that controls presynaptic differentiation. *Nature* 430: 345–350.
 88. Rohrbough J, Kent KS, Broadie K, Weiss JB (2012) Jelly belly trans-synaptic signaling to anaplastic lymphoma kinase regulates neurotransmission strength and synapse architecture. *Developmental neurobiology* 73(3):189–208.
 89. The I, Murthy AE, Hannigan GE, Jacoby LB, Menon AG, et al. (1993) Neurofibromatosis type 1 gene mutations in neuroblastoma. *Nature genetics* 3: 62–66.
 90. George RE, Sanda T, Hanna M, Frohling S, Luther W, 2nd, et al. (2008) Activating mutations in ALK provide a therapeutic target in neuroblastoma. *Nature* 455: 975–978.
 91. Chen Y, Takita J, Choi YL, Kato M, Ohira M, et al. (2008) Oncogenic mutations of ALK kinase in neuroblastoma. *Nature* 455: 971–974.
 92. Janoucix-Lerosy I, Lequin D, Brugieres L, Ribeiro A, de Pontual L, et al. (2008) Somatic and germline activating mutations of the ALK kinase receptor in neuroblastoma. *Nature* 455: 967–970.
 93. Mosse YP, Laudenlager M, Longo L, Cole KA, Wood A, et al. (2008) Identification of ALK as a major familial neuroblastoma predisposition gene. *Nature* 455: 930–935.
 94. Holzel M, Huang S, Koster J, Ora I, Lakeman A, et al. (2010) NF1 is a tumor suppressor in neuroblastoma that determines retinoic acid response and disease outcome. *Cell* 142: 218–229.
 95. Stoica GE, Kuo A, Powers C, Bowden ET, Sale EB, et al. (2002) Midkine binds to anaplastic lymphoma kinase (ALK) and acts as a growth factor for different cell types. *The Journal of biological chemistry* 277: 35990–35998.
 96. Mashour GA, Wang HL, Cabal-Manzano R, Wellstein A, Martuza RL, et al. (1999) Aberrant cutaneous expression of the angiogenic factor midkine is associated with neurofibromatosis type-1. *The Journal of investigative dermatology* 113: 398–402.
 97. Mashour GA, Ratner N, Khan GA, Wang HL, Martuza RL, et al. (2001) The angiogenic factor midkine is aberrantly expressed in NF1-deficient Schwann cells and is a mitogen for neurofibroma-derived cells. *Oncogene* 20: 97–105.
 98. Mashour GA, Driever PH, Hartmann M, Drissel SN, Zhang T, et al. (2004) Circulating growth factor levels are associated with tumorigenesis in neurofibromatosis type 1. *Clinical cancer research: an official journal of the American Association for Cancer Research* 10: 5677–5683.
 99. Katayama R, Shaw AT, Khan TM, Mino-Kenudson M, Solomon BJ, et al. (2012) Mechanisms of acquired crizotinib resistance in ALK-rearranged lung Cancers. *Science translational medicine* 4: 120ra117.
 100. Li W, Ohlmeier JT, Lane ME, Kalderon D (1995) Function of protein kinase A in hedgehog signal transduction and *Drosophila* imaginal disc development. *Cell* 80: 553–562.
 101. Johnson KG, Tenney AP, Ghose A, Duckworth AM, Higashi ME, et al. (2006) The HSPGs Syndecan and Dallylike bind the receptor phosphatase LAR and exert distinct effects on synaptic development. *Neuron* 49: 517–531.
 102. Loya CM, Lu CS, Van Vactor D, Fulga TA (2009) Transgenic microRNA inhibition with spatiotemporal specificity in intact organisms. *Nature methods* 6: 897–903.
 103. Huang S, Laoukil J, Epping MT, Koster J, Holzel M, et al. (2009) ZNF423 is critically required for retinoic acid-induced differentiation and is a marker of neuroblastoma outcome. *Cancer cell* 15: 328–340.
 104. Rewitz KF, Yamanaka N, Gilbert LI, O'Connor MB (2009) The insect neuropeptide PTTH activates receptor tyrosine kinase torso to initiate metamorphosis. *Science* 326: 1403–1405.